Project Number: MQP YW1 – YW1

Developing an Ultra-High Energy Density Flow Battery

A Major Qualifying Project Submitted to the Faculty of

WORCESTER POLYTECHNIC INSTITUTE

In partial fulfillment of the requirements for the

Degree in Bachelors of Science

By

Daniel Irizarry

Tung Ton

Kemal Yorulmaz

Date: March 27, 2015
Approved by:

Professor Yan Wang, Advisor

Professor Alexei A. Zozulya, Co-Advisor

Abstract

Energy storage systems are necessary to meet the increasing energy demand. Flow batteries with their independence in power and energy, long cycle life, and low maintenance are attractive for energy storage applications. This project's goals are to design and build a high power density Nickel-Zinc flow battery. Nickel and Zinc suspensions have energy densities of 162.35 (Wh/L) and 422.24 (Wh/L) respectively. The battery (cell) is composed of two multichannel plates and separators, with each plate having 10 channels. Two types of suspensions were prepared and injected into the plates' channels and the cell was then tested by several charging and discharging cycles to obtain the performance characteristics of the battery.

Executive Summary

With a rapid increase in the use of renewable energy sources, there is an increasing desire for large-scale grid storage systems. Current storage systems are very expensive and have limited life spans, so flow batteries are an attractive alternative for storage applications due to their long cycle life. However, current flow batteries have mediocre performances. Their energy density is low due to the solubility limit of active materials in the chemical solutions. Also, they offer low power density since the effective surface area of the electrodes used in flow batteries is small. In addition, the cost of the materials and manufacturing processes are very high. Therefore, our goal for this project was to develop a new type of battery that offers better performance and lower cost.

A flow battery is a fully rechargeable energy storage device that converts stored chemical energy into electrical energy. The main advantage of the flow battery is the separation of power and energy. Energy is determined by the volume of the electrolyte which is stored in separate tanks, whereas power is determined by electrochemical cells.

In order to achieve our goal, three separate objectives were determined: designing, manufacturing, and testing of our flow battery prototype. The design includes 10 channels on the top surface of the electrodes where chemical reactions take place. In addition, on the sides of the electrodes, there are two deep holes where the suspension goes in, flow through the channels and exit the electrode. In the manufacturing part, in order to machine our electrode to their proper dimensions and shape, manufacturing operations were created. Contouring operations for the lateral dimensioning and the lowered edge, facing operations for the bottom and top surface dimensioning, pocketing operations for the channels, and drilling operations for the holes, were used.

In the testing stage, anode electrolyte mixture and cathode electrolyte mixture were prepared separately. The electrolyte mixtures include anode and cathode charging materials, carbon powder, a chemical agent and an electrolyte. A grinder and a sonic vibrator were used to lower the size of the

materials and to homogenize the electrolyte mixture, respectively. With the help of the connectors and tubes, the anode and the cathode electrolyte mixtures were filled into the electrodes and crocodile clips were connected to the current collector attached to the electrodes. With this, electrons moved through an external circuit which was connected to a battery channel analyzer and a computer to obtain charging and discharging performance characteristics of our flow battery prototype.

In conclusion, although our flow battery works well without any leakage or choked issues, the testing results were not as good as the theoretically calculated results. Therefore, further testing is recommended to obtain more reliable results and to prove the high potential of this technology.

Acknowledgements

We would like to acknowledge and thank our Worcester Polytechnic Institute advisors Professor Yan Wang and Professor Alexei Zozulya for providing great assistance and feedback throughout our Major Qualifying Project.

We would also like to show our appreciation to Jin Liu, a PhD student at Worcester Polytechnic Institute for his continued guidance and support in the laboratory experiment during our project.

Table of Contents

Table of Figures

Table of Tables

1.0 Introduction

The global energy consumption is expected to rise 41 percent from 2012 to 2035 (1.5% a year), according to BP Energy Outlook 2035. Traditional source consumption like Oil, Gas, and Coal are expected to grow 0.8%, 1.9%, and 1.1%, respectively. By 2035, each of these traditional sources is expected to cover around 26-27% of the energy market. Nuclear energy and hydroelectric powers are each expected to grow nearly 2% (1.9% and 1.8% respectively). Renewable energy is currently the fastest growing energy production source in the market (6.4 % a year) and by 2035, these non-fossil fuels sources share around 5-7% each. [1] With this ample increase in the world's energy consumption, efficient energy storage is a crucial aspect to achieve in order to meet the high energy demand the future entails.

A viable and beneficial method to store energy are with flow batteries. Flow batteries can be used to store energy on a grid, capturing the energy generated with traditional methods such as gas and oil, but more importantly, being able to store renewable energy generated by solar and wind farms. They have a variety of applications such the ones mentioned, and have the potential be used in hybrid and electric vehicles. Flow batteries are the future when it comes to clean energy storage.

The goal of our project was to design and manufacture a multichannel flow battery cell than can be used as a building block to further improve on this new technology. Our design will serve its purpose in testing the chemical suspension used and to analyze the charging and discharging performance of our design, in order to obtain essential information to further improve the design.

2.0 Background Research

Energy storage technology development is important to meet the increasing global demands of energy. Flow batteries are a new type rechargeable battery that can be used to store electrical energy on the grid scale. Currently, flow batteries have energy densities of around 25 Wh/kg which is relatively low compared to other traditional batteries such as lead-acid and Li-ion batteries. [20] However, with research aiming to increase the batteries energy density and efficiency, the usage of flow batteries for energy storage is expected to increase in the future.

2.1 Energy Storage Methods

The storage of energy involves converting one form of energy to another, such as potential energy to electrical energy, chemical energy to electrical energy, etc. Energy storage is necessary to make energy usage feasible (electric cars, portable electric devices). The usage of energy fluctuates depending on time so energy storage is needed to increase energy security and efficiency. Furthermore, renewable energy sources such as solar, wind, etc. fluctuates depending on seasons and vary between day and night so the storage of these types of energy is necessary to increase the efficiency and provide continuous energy power. Some energy storage methods are presented below.

2.1.1 Pumped Hydroelectric Power

With Pumped Hydroelectric energy storage, energy is stored in the form of gravitational energy of water. A schematic diagram of a pumped hydroelectric power is shown in Figure 1. The excess electricity (during low energy demand hours, or excess energy from solar, wind plants) is used to pump water from the lower reservoir to the upper reservoir. When electricity is in high demand, water is flowed from the upper reservoir through a turbine to the lower reservoir to generate electrical energy. Pumped Hydroelectric energy systems can provide reliable energy and large scale storage capacities.

The maintenance and operating cost of this method are low and the round trip efficiency can reach 80%.[2]

The energy stored in water is given by the following equation:

$$E = mgh;$$

where m is the mass of water, g is the gravitational acceleration and h is the average height.

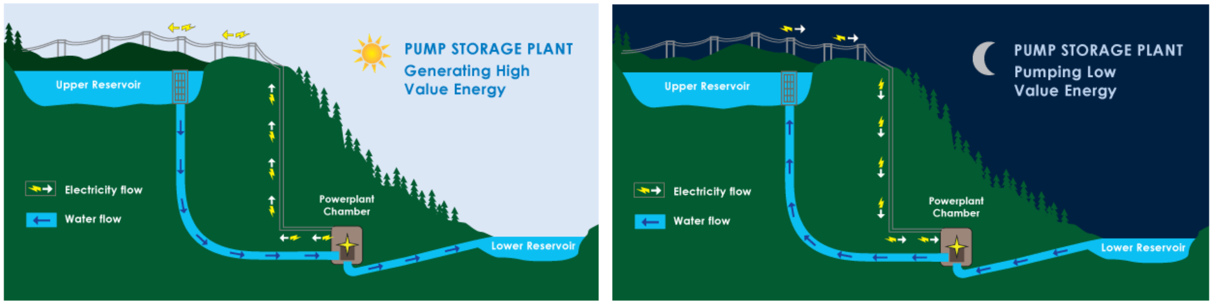

Figure 1 : Schematic of pumped hydroelectric power. [3]

2.1.2 Compressed Air

Compressed Air storage facilities store energy in the form of compressed air. A schematic diagram of a compressed air storage system is shown in Figure 2. A compressor is used to compress a gas, and a turbine is used to convert energy from compressed gas to electrical energy. Like Pumped Hydroelectric systems, this method can be used in large scale energy storage applications. The energy density that can be achieved by compressed air storage is low compared to batteries, so there are limitations in small scale applications like electric and hybrid vehicles. [4]

The energy stored in compressed air (in KJ per m^3) is approximated by the following equation:

$$\frac{E}{V} = 100 * \ln\left(\frac{P_f}{P_i}\right);$$

where P_f and P_i are the pressures of gas, E is the energy, and V is the volume.

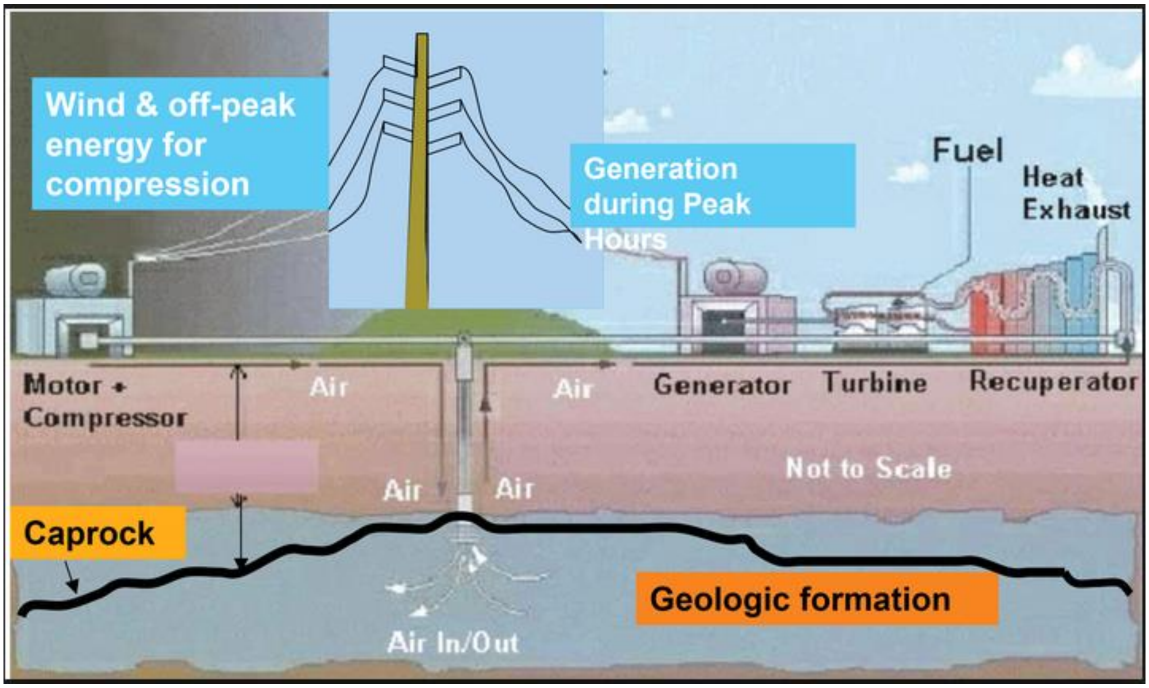

Figure 2: Schematic of a compress air storage system. [5]

2.1.3 Flywheels

Flywheels storage systems store energy in the form of rotational kinetic energy. A diagram of a Flywheel Energy Storage System is shown in Figure 3. Flywheel is a rotating mechanical device that is used to store energy. Energy is transferred to the flywheel by applying a torque which then releases the stored energy by applying torque to a mechanical load. The flywheel is used to supply energy to a system when the energy source is not continued. Another possible application is that it can store energy in a vehicle where energy can be applied during braking and extracted when needed. The flywheel is compacted and can be combined to increase total energy storage capacities and has a high efficiency (80-90%). [6]

The energy storage in a flywheel system depends on the geometry of the device, its mass and rotational frequency. The energy stored in flywheels can be calculated with the following equation:

$$E = \frac{1}{2} I \omega^2;$$

where $\omega = 2\pi f$ is the angular velocity, and I is the moment of inertia, which depends on the geometry and mass of the device.

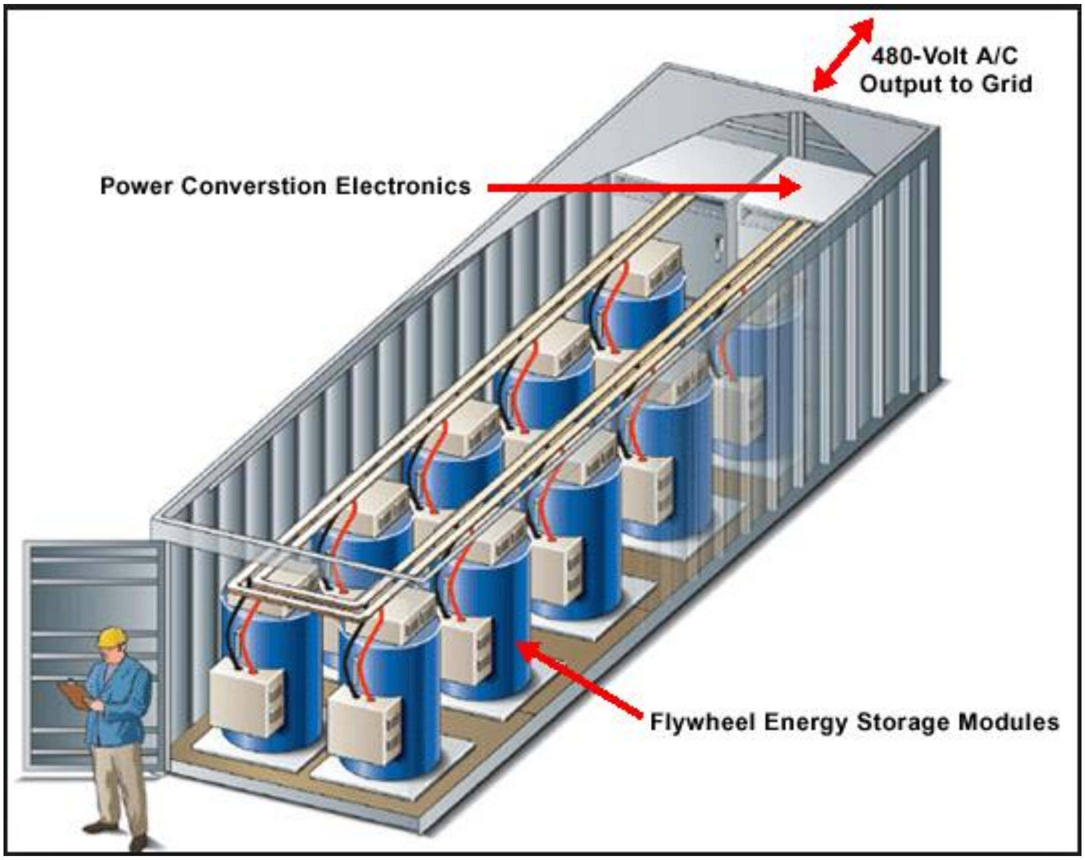

Figure 3: Flywheel energy storage system. [7]

2.1.4 Superconducting Magnetic Energy Storage (SMES)

Superconducting Magnetic Energy Storage (SMES) system stores energy in the form of magnetic fields. In SMES systems, electric current is injected into a non-electrical resistant coil which would circulate indefinitely until needed. The energy can be released by discharging the coil and the time it takes to charge and discharge is very short. Currently, application for large scale storage is not feasible due to limitation in technology, though this method has very high energy efficiency (95%). [8]Figure 4 depicts a basic structure of a SMES device.

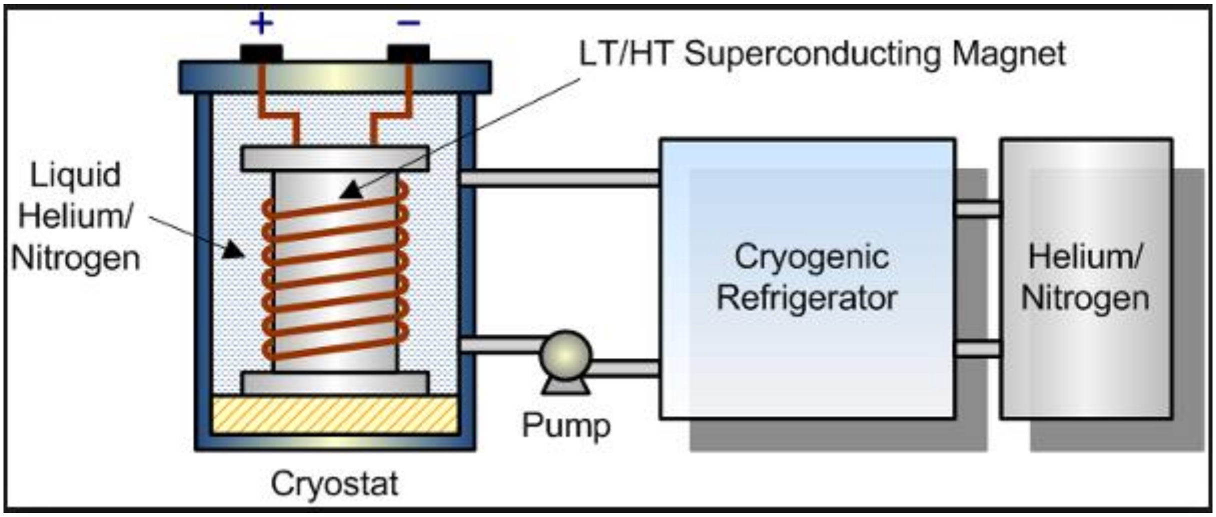

Figure 4: Basic structure of a SMES device. [9]

Superconducting magnets are characterized by a critical temperature Tc; at this temperature, the electrical resistivity equals zero. High-temperature superconducting materials are relatively popular. Electricity derived from SMES is in the form of direct current (DC), so in some cases an AC (alternative current) –DC conversion system is needed.

The energy stored in a coil is given by the following equation;

$$E = \frac{1}{2} L I^2;$$

where L is the inductance of the coil, which depends on the coil dimension, number of turns of wire and material, and I is the current.

2.1.5 Batteries

A battery is a device that converts stored chemical energy to electrical energy. A battery may have one or more cells, each having three components: an anode, a cathode, and an electrolyte. Batteries can be classified as rechargeable or non-rechargeable. The latter is suitable for devices that use little power such as watches, flashlights, and calculators. Rechargeable batteries are usually suitable for energy stored and electric vehicles. [10]

The energy contained in a battery depends on the size and the battery's chemistry. The cost of electricity derived from batteries is very high (for Non-rechargeable AAA batteries, the electricity cost is around $900 per KWh or 8000 times the cost of electricity from an outlet). However, batteries are portable sources that can be used in electronic devices such as cell phones, cameras, flashlights, etc. [11] Figure 5 is a side by side comparison of several different batteries.

Figure 5: A side by side comparisons of several batteries. [12]

2.2 Flow Batteries

This new type of battery is very attractive for large scale applications. They can serve as back-up power systems and can store energy at the grid scale. The flow battery is charged and discharged by chemical reactions between the two liquid electrolytes of the battery. The liquid electrolytes are stored externally in two tanks. The size and properties of electrolytes determine the battery energy capacity while the sizes of electrodes determine the battery power capacity. A flow battery system consists of many parts: pipes to connect electrolytes to storage tanks and cells stacks, pumps to circulate the electrolytes through the cells stacks, and heat exchangers to maintain the operating temperature of the electrolytes. During operation, electrolytes are pumped through the cells where they undergo chemical reactions and create electrical energy. Figure 6 shows a schematic diagram of a flow battery.

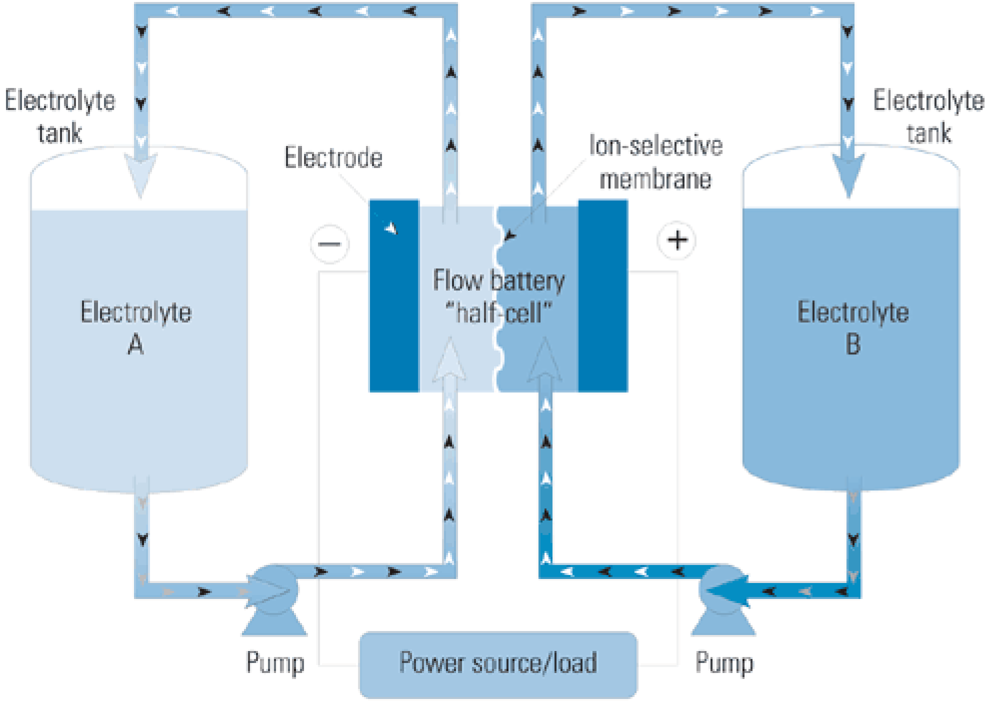

Figure 6: Schematic diagram of Flow Battery. [13]

Table 1 list the characteristics of flow batteries compared to other storage systems. The table shows that flow batteries with typical power around 100 KW to 10 MW and typical energy around 1 to 100MWh are suitable for medium to large scale applications.

Table 1: Characteristic of Flow Batteries compared to other storage systems. [14]

	Typical Power	Typical Energy	Typical duration discharge	Maturity
Batteries (lead-acid, NiCd, NiMH, Li-ion)	kW – 500 kW	MWh – 100 MWh	1 h – 8 h	Mature
Flywheels	500 kW – 1 MW	100 kWh – 100 MWh	< 5 minutes	Mature
Pumped hydro	100 MW – 4000 MW	500 MW - 15 GWh	4 – 12 h	Mature
CAES	25 MW – 3000 MW	200 MWh - 10 GWh	1 – 20 hours	Developed, first generation demonstrated
NaS	1 MW	1 MWh	1 hour	Developed, stage of demonstration projects finished, commercially available
SMES	10 kW – 10 MW	10 kWh – 1 MWh	1 – 30 minutes	Developed, not commercial yet
Supercapacitors	< 250 kW	10 kWh	< 1 minute	Developed
Flow batteries	100 kW – 10 MW	1 – 100 MWh	10 hours	Developed, stage of demonstration projects
Hydrogen storage	10 MW	unlimited	> 5 hours	Developing

2.2.1 Advantages and Disadvantages

Similar to other types of batteries, flow batteries have benefits and drawbacks. The following sections list the main advantage and disadvantage of flow batteries.

Advantages:

- The power capacity (depends on the size of electrodes) and the energy capacity (depends on the size of the external storage tanks) of flow batteries are independent. This allows the design to meet the specific needs of applications.
- The electrodes only collect current and are not involved in chemical reactions; hence they are stable and durable.
- Flow batteries have the ability to discharge and recharge without affecting the cycle life.
- Flow batteries have long cycle life and low maintenance.

Disadvantages:

- Flow batteries systems are complex. They require pumps, sensors, flow and power management, and secondary containment vessels.
- The energy densities of flow batteries are usually low compared to other types of batteries.

2.2.2 Types of Flow Batteries

There are three popular types of flow batteries: Vanadium Redox Batteries (VRB), Polysulphide Bromide Batteries (PSB), and Zinc Bromine (ZnBr). PSB focuses on multi-MW systems, while VRB and ZnBr have typical ranges below 1 MW. [15] Table 2 shows the comparison of those types of flow batteries based on the current status.

1. Vanadium Redox Batteries (VRB)

Vanadium Redox Batteries use two Vanadium electrolytes (V2+/V3+ and V4+/V5+), and H+ ions are exchanged between the two electrolytes through a membrane.

The reactions during the charging process are as followed:

$$V^{3+} + e^- \rightarrow V^{2+},$$

$$V^{4+} \rightarrow V^{5+} + e^-;$$

and during the discharging process the reactions are reversed.

2. Polysulphide Bromide Batteries

Na_2S_2 (Sodium Sulphide) and $NaBr_3$(Sodium Tribromide) are used as electrolytes. The Na+ ions passes through the membrane during the charging or discharging process.

The reactions during the charging process are as followed:

$$2Na_2S_2 \rightarrow Na_2S_4 + 2Na^+ + 2e^-,$$

$$NaBr_3 + 2Na^+ + 2e^- \rightarrow 3NaBr;$$

and during the discharging process the reactions are reversed.

3. Zinc Bromine (ZnBr)

Solutions of Zinc and a complex Bromine compound are used as electrodes.

The reactions during the charging process are as followed:

$$Zn^{2+}_{aq} + 2e^- \rightarrow Zn_s,$$

$$2Br^-_{aq} \rightarrow Br_{2(aq)} + 2e^-;$$

and during the discharging process the reactions are reversed.

Table 2: Comparison of Flow Batteries based on current status. [16]

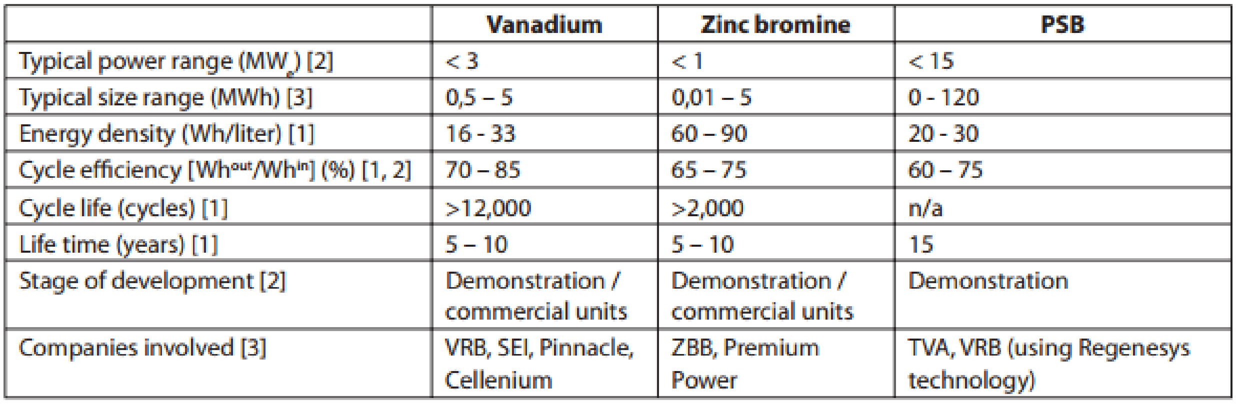

	Vanadium	**Zinc bromine**	**PSB**
Typical power range (MW_e) [2]	< 3	< 1	< 15
Typical size range (MWh) [3]	0,5 – 5	0,01 – 5	0 - 120
Energy density (Wh/liter) [1]	16 - 33	60 – 90	20 - 30
Cycle efficiency [Wh^{out}/Wh^{in}] (%) [1, 2]	70 – 85	65 – 75	60 – 75
Cycle life (cycles) [1]	>12,000	>2,000	n/a
Life time (years) [1]	5 – 10	5 – 10	15
Stage of development [2]	Demonstration / commercial units	Demonstration / commercial units	Demonstration
Companies involved [3]	VRB, SEI, Pinnacle, Cellenium	ZBB, Premium Power	TVA, VRB (using Regenesys technology)

2.2.3 Applications of Flow Batteries

The energy storage market is expected to reach €15 billion in 2020 and to be €26 billion in 2030. [17] Flow batteries are good candidates for large scale energy storage. Flow batteries can provide high power and high energy capacity. Furthermore, they have low operating cost and can be charged rapidly. Hence, flow batteries are suitable for applications such as load balancing, storing renewable energy, electric vehicles, and peak saving.

Load balancing refers to the storage of excess energy from grid or renewable energy sources during peak time and are released when the demands are high. This will increase the reliability of the system. Flow batteries can be discharged and charged up to 10,000 times without replacing the membrane and the electrolytes never require replacement. [18]

Renewable energy derived from solar and wind energy systems fluctuate, so flow batteries can be used to store these types of energy and serve as a means of back-up, hence, creating a steady and reliable energy supply from renewable sources. Also it can be used as back up power when the main power supply fails to provide energy.

Flow batteries are attractive for their applications in electric vehicles; they can instantly be “recharged” by removing used electrolyte mixtures and replaced with new electrolyte mixtures (the process is like filling the tank with gas). This is the advantage over traditional Li-ion batteries; furthermore, flow batteries may have lower operating costs per kilometer. [18]

Another application of flow batteries is peak saving. Heavy electric users can charge a battery during low demand for cheaper energy cost and discharge the battery during peak time to avoid more expensive costs.

2.2.4 Current large scale energy storage systems

Currently, flow batteries are at the early commercial state. According to a report from Lux Research, Redox flow batteries will carve out a 360 MWh market in 2020 worth $190 million from $100 million in 2014. The overall battery industry will reach a $46.5 billion market in 2023 from a $20.1 billion market in 2014. [19] The percent market share of flow batteries is not expected to increase in the near future. The sample of flow battery installations and proposed projects are listed below[20]:

- a 1.5 MW UPS system at Japan
- a 275 kW output balancer at Hokkaido
- a 200 kW at the Huxley Hill Wind Farm on King Island, Tasmania
- a 250 kW at Castle Valley, Utah
- a 12 MW·h (43 GJ) at the Sorne Hill wind farm, Donegal, Ireland,

and the proposed projects of flow battery installations are listed below:

- a 60MWh redox flow battery (RFB) order in Japan (to add increasing amounts of renewable energy to its grid, which serves millions of customers in the northernmost area of Japan's four major islands,)[21]
- a 1.26MWh Energy Storage for remote Scottish wind farm(The proposed 1.26MWh VRFB storage system will be located on the island of Gigha, which has limited connection to the mainland via an ageing subsea cable). [22]

2.2.5 History Development, Current state of Technology, and Challenges

Flow batteries were invented by the French scientist Charles Renard in 1884. However, there was not much research in flow batteries until the 1970's. Early flow batteries had limitations such as chemical reaction taking place at high temperatures and pressure; and they used hazardous chemicals. Vanadium Redox Flow Battery was invented at the University of New South Wales in 1984. [23]

Currently, Vanadium Redox flow batteries (VRB) have energy densities of about 25 Wh/kg (this is relatively low compared to other rechargeable batteries such as lead-acid, which has an energy density range of 30-40 Wh/kg; and lithium ion having an energy density range of 80-200 Wh/kg), charge/discharge efficiency of 75-80%, life span of 10-20 years, cycle durability greater than 10,000 cycles, and a cell voltage range of 1.15-1.55 V. [20]

Flow batteries are reliable and have low maintenance fees; electrolytes last indefinitely and have a long membrane life, and zero emissions. A new modular stack design and construction allows the basic module to be built into multiple array systems with a wide range of power and capacity. [24] Currently, the overall system price is around $350 to $600 per kWh for sizes ranging from a few hundred kW to MW size systems. But with a larger system, the price is expected to decrease. [20]

Prudent Energy's large-scale systems are built on a 175 kW modular basis allowing for easy scaling to obtain a multi-megawatt size with very high availability rates, essential for utility applications. [20] Renewable Energy Dynamics Technology Ltd (REDT) has developed a series of Vanadium Redox Batteries with a range of 30 kWh to 180 kWh. These products are expected to discharge down to 0% and charge up to 95% without causing degradation for 10,000 cycles; they are also safe, environmentally friendly, and only require annual maintenance checks. They claim that it is possible to build 5MWh Vanadium Redox battery systems using many stacks. [24] There are other reputed companies such as V-Fuel Pty Ltd, Australia; Cellstrom, Austria; and the Cellennium Company Limited, Thailand.

There are differences between flow batteries cell costs and flow batteries projects prices. Flow batteries occupy large areas compared to other batteries; space requirements for flow batteries could be as high as 30% of the total system cost. In addition, flow batteries require complex support systems such as pumps, sensors, tanks, etc, and have low energy densities. Increasing the electrolyte concentration will increase the energy density, but will also increase the flammability. [25]

The US Department of Energy set long-term targets for battery storage technologies for RFBs: a capital cost of $150 per kWh and a system efficiency of over 80%. However, the most developed VRB system cost about $500 per kWh because of its dependence on expensive Vanadium, ionic exchange membranes, and other components. [26]

Studies on the operational parameters (such as electrolyte concentration, current density, temperature, etc.) and research on electrodes, ion exchange membranes, cells, stacks and system designs are necessary to increase the power density, improve the performance and the economic value of flow battery technologies. [26]

3.0 Basic Principles of Physics behind Flow Batteries

Flow batteries are fully rechargeable energy storage devices which are referred to as electrochemical or galvanic cells as they store electrical energy in the form of chemical energy and they drive electrical energy from spontaneous redox reactions taking place within the cell. In general, when a flow battery is connected to an external power source, it is charged by the source and a finite charge Q is stored. This way, during the charging process, electrical energy is converted into chemical energy. On the other hand, when a flow battery is connected to an external resistive circuit, finite charge Q is released which results in the movement of electrons that creates current through the external circuit. Thus, during the discharging process, chemical energy is converted into electrical energy. [29]

3.1 Redox Reactions

Redox Reactions consist of chemical reactions where atoms change their oxidation number. Redox reactions in electrochemical cells involve the transfer of electrons between the electrolyte mixture and electrode. They can be represented as two separate concepts known as oxidation and reduction. During the oxidation reaction, there is an increase in the oxidation number of an atom as the atom loses an electron. On the other hand, during the reduction reaction, there is a decrease in the oxidation number of an atom as the atom gains an electron. [30] The oxidation alone and the reduction alone are each called a half reaction. Thus, two half-reactions occur together to obtain a balanced reaction.

The two parts of redox reactions are shown below:

1. Reduction Reaction:

$$\text{Oxidant} + e^- \longrightarrow \text{Product}$$

2. Oxidation Reaction

$$\text{Reductant} \longrightarrow \text{Product} + e^-$$

In our electrochemical cell, the overall reaction is the sum of the two half reactions. Therefore a standard voltage of 1.73 V is produced by the following half reactions:

Half Reactions	Potential, E
$\mathrm{2NiOOH + 2H_2O + 2e^-} \underset{\text{charge}}{\overset{\text{discharge}}{\rightleftharpoons}} \mathrm{2Ni(OH)_2 + 2OH^-}$	0.49V
$\mathrm{Zn + 2OH^-} \underset{\text{charge}}{\overset{\text{discharge}}{\rightleftharpoons}} \mathrm{Zn(OH)_2 + 2e^-}$	1.24V

Overall Reaction	
$\mathrm{2NiOOH + 2H_2O + Zn} \underset{\text{charge}}{\overset{\text{discharge}}{\rightleftharpoons}} \mathrm{2Ni(OH)_2 + Zn(OH)_2}$	1.73V

The net cell potential is as follows:

$$E_{net} = -\Delta \frac{G_{net}}{nF} = 1.73\ \mathrm{V};$$

where G_{net} is the Gibbs Free Energy, n is the number of moles and F is the Faraday constant. As the Gibbs free energy is negative considering the net cell potential of our flow battery, reaction is spontaneous. The following figure below shows how ion transfer and electron transfer occurs in an electrochemical cell during the oxidation and reduction reaction.

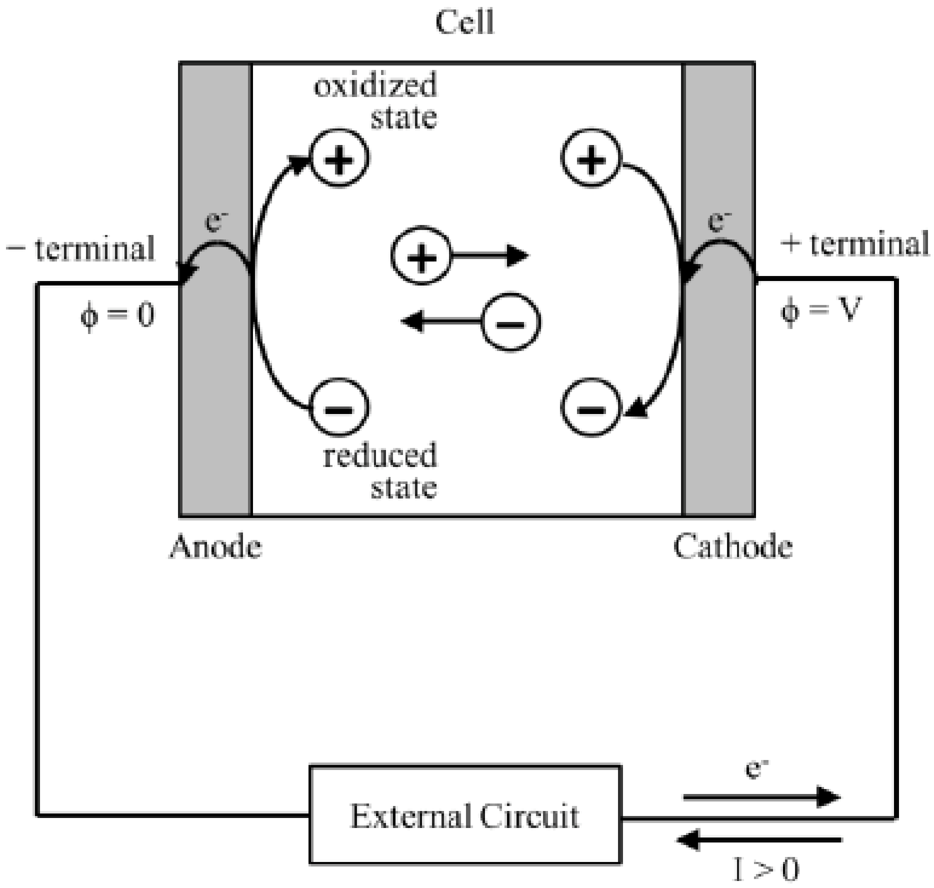

Figure 7: Galvanic Operation of an Electrochemical Cell. [31]

3.2 How a Flow Battery Works

The mechanism of a flow battery is very similar to a conventional battery. The major difference is the separation of power and energy. In conventional batteries, electrochemical cells have fixed quantities of charge materials so both storage of electrolyte mixtures and chemical reactions occur at the same place. Thus, electrochemical cells determine both power and energy. However, in flow batteries power is determined by electrochemical cells and energy is determined by the volume of electrolyte mixture, which is stored in separate tanks. The separation of power and energy provides design flexibility. In a flow battery, electrochemical stack size can be modified according to the desired power output and size of the storage tanks can be adjusted considering the energy storage need of the specific application. The following figure shows the configuration of a flow battery.

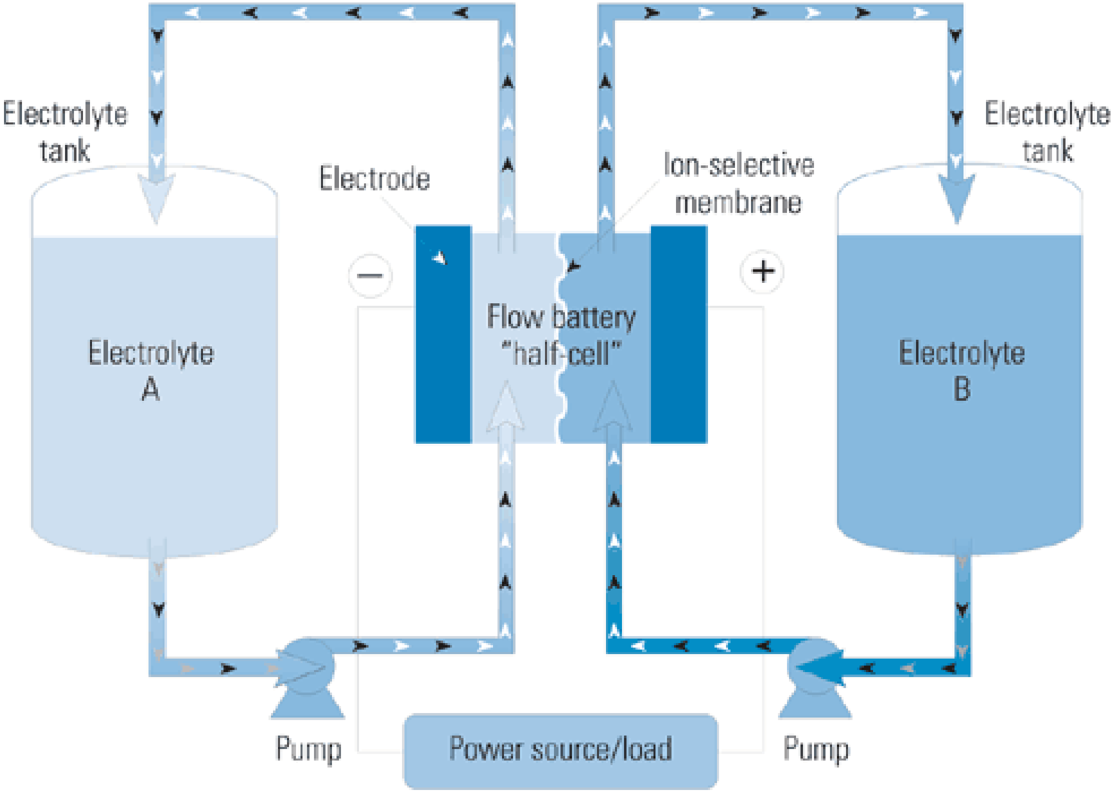

Figure 8: Schematic diagram of Flow Battery. [13]

Electrolyte mixtures are stored in separate tanks. During operation, electrolyte mixtures are pumped through the electrochemical cell where chemical reactions takes place. An electrochemical cell consists of two half-cells. Each half-cell includes an electrode and electrolyte mixture. Although electrodes do not touch each other, they are electrically connected to each other by the electrolyte mixture. During discharge, an electron is released via an oxidation reaction from the negative side of the battery while ions pass through the ion exchange membrane which separates half cells from each other.[32] Thus, ion selective membranes prevent the mixing of the electrolytes. The electrons released pass through the electrode and travel through an external circuit where the movement of electrons create current. The total difference between the standard electrode potentials of the anode and cathode side of the electrochemical cells determine the electromotive force (Voltage) generated.[33] Therefore since $\text{Power} = \text{V} * \text{I}$, we can obtain a power output to deliver electrical energy to the specific load. On the other hand, an electron is accepted via a reduction reaction on the positive side of the electrochemical cell. The directions of the current and the chemical reactions are reversed during the charging process. [32] So during the discharging process the negative electrode is the anode where oxidation reaction occurs. However, during the charging process, it turns into the cathode where reduction takes place.

3.3 Understanding of Current and Voltage in Flow Batteries

The following figure shows an equivalent circuit in rechargeable batteries.

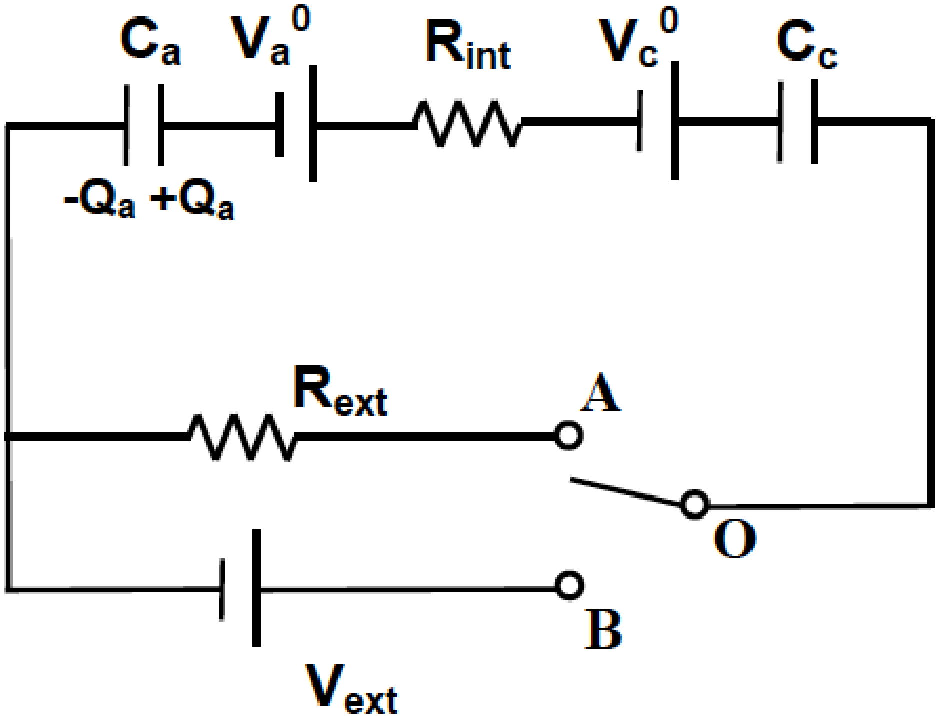

Figure 9: Equivalent Circuit of Rechargeable Batteries. [29]

During the discharging process OA is connected in the equivalent circuit diagram and in order to analyze the discharging process, first we need to introduce Capacitance:

$$C = \frac{Q}{V},$$

where C is the capacitance(in Farads), Q is the amount of charge (Coulombs), and V is the voltage (Volts) across the electrode. The following equations show the total voltage calculations:

$$Total\,Voltage = Voltage_{resistor} + Voltage_{electrodes}$$

$$Total\,Voltage = i(R_{int} + R_{ext}) + \frac{Q_{anode}}{C_{anode}} + \frac{Q_{cathode}}{C_{cathode}}$$

where,

$$R_{int} = R_{anode} + R_{electrolyte} + R_{cathode}$$

and Current can be calculated as follows:

$$Current = I = -\frac{Q_{anode}}{(R_{int}+R_{ext})C_{anode}} - \frac{Q_{cathode}}{(R_{int}+R_{ext})C_{cathode}} + \frac{V}{(R_{int}+R_{ext})}.$$

By applying Kirchoff’s Voltage Law which states that the sum of the electrical potential differences around any closed network is zero, we obtain:

$$Cell\,Voltage = V = I * R_{ext} = I * R_{int} = emf,$$

by obtaining values for current and cell voltage, we can calculate the electrochemical cell power, P, which can be stated as the electrical work done by the electrochemical cell per unit time. As the electrons move from the anode electrode to the cathode electrode, electric field is doing the work.

Therefore,

$$dW = dQ(V_{anode}^0 - V_{cathode}^0)$$

$$\frac{dW}{dt} = \frac{dQ}{dt}(V_{anode}^0 - V_{cathode}^0)$$

where the power $\left(\frac{dW}{dt}\right)$ is the current that battery produces times the potential difference of the electrodes. Finally we can represent Power as follows:

$$Power = Current * Cell\,Voltage = IV.$$

3.4 Capacity and Discharge Characteristics of Flow Batteries

The Peukert's Law estimates the efficiency factor of a battery during discharge by using the internal resistance and the recovery rate of a battery. Thus, we have formula that expresses the relationship between current, discharge time, and capacity for a flow battery, as follows: [34]

$$t = \frac{Q_p}{I^k}$$

where Q_p is the capacity when discharged at a rate of 1 amp, I is the current drawn from battery (A), t is the amount of time (in hours) that a battery can sustain, and k is a constant around 1.3.

Capacity (A*h) of a flow battery can be expressed as the amount of electric charge available when the battery is discharged at a certain discharge current. Therefore, by increasing the size of the electrode, it is possible to obtain greater charge capacity. Also, there are many factors affecting the stored charge capacity of a flow battery such as internal energy losses and terminal voltage. [35]

The C-rate of a flow battery can be described as the rate at which it is discharged considering its total capacity. One C-rate means that the applied discharge current will discharge the total capacity of the battery in one hour. Therefore, C-rate is inversely proportional to the number of electrons produced per unit of time. [35]

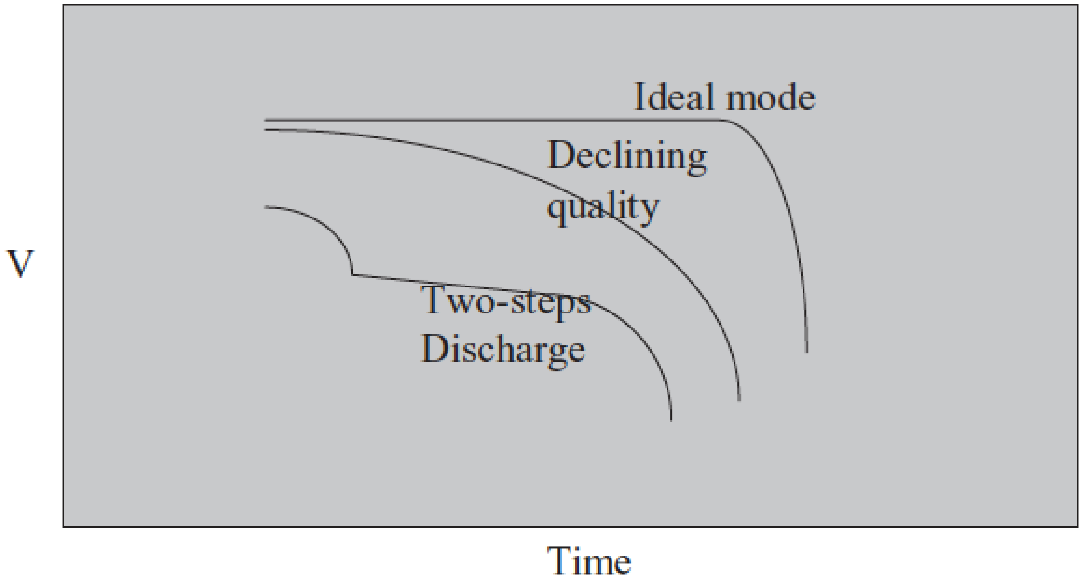

Figure 10: Change of voltage with time behavior in different cells [33]

The discharge figure shown above demonstrates a plot of the voltage against the time during the discharging process. The ideal mode is desirable in flow batteries where the voltage remains constant as the battery's charge capacity is used. In the ideal mode, the voltage remains constant with time until the charge capacity is fully used and then voltage drops to a lower level. [33]

3.5 Properties of Materials in our Prototype

This section includes chemical and physical aspects of materials used in our prototype. It also covers the roles of the materials in order to keep the battery system working without any failures.

3.5.1 Electrodes

Electrodes only collect electrons and are not involved in chemical reactions so they are durable. The electrodes have conductivity laterally and perpendicularly to the electrolyte flow. We used Nickel and Copper electrodes in our flow battery prototype. Nickel is a hard, ductile, and malleable metal that can be worked hot or cold to fabricate many items. It is a poor conductor of electricity, good conductor of heat and it is magnetic. In addition, it work hardens during manufacturing processes so the Nickel material becomes stronger as it is induced by stresses. Nickel offers excellent protection from corrosion from air and seawater. It is also an excellent alloy metal so we used Nickel 200 Alloy as the material of the electrode in one half cell which is 99% pure Nickel and the remaining elements are Carbon, Copper, Iron, Manganese, Silicon, and Sulfur.[36] On the other hand, Copper is ductile, malleable, and easily formed into desired shapes. It has high resistance to weak acids and it resists atmospheric corrosion. It has high resistance to corrosion due to the bluish-green film (patina) that is formed over its surface when copper is exposed to seawater or moist air. In addition, Copper is an excellent conductor of electricity and heat. [36]

3.5.2 Charge Materials

In our flow battery, Zinc Oxide (ZnO) is employed as the anodic (anode) charge material and Nickel Hydroxide ($Ni(OH)_2$) is employed as the cathodic (cathode) charge material. Zinc Oxide is insoluble in water. It is a broad energy gap semiconductor (3.37 eV) with properties of high electron mobility and has an ability to sustain large electric fields. [37]On the other hand, Nickel (II) Hydroxide has strong redox properties so it is used in rechargeable electrodes. It is an insoluble compound and undergoes oxidation to Nickel (III) Oxide-Hydroxide. [36]

3.5.3 Electrolyte

Potassium Hydroxide was used as the material of electrolyte in our prototype. It helps the movement of ions during the chemical reactions in flow batteries. It contains varying amounts of water and its dissolution in water produces heat. Potassium Hydroxide is preferred as the electrolyte material as it has high conductivity.

3.5.4 Stabilizing Agent

Combination of Carbon Powder and a chemical agent forms a stabilizing agent. Thus, stabilizing agent avoids settling of the suspension and stabilizes suspension. Carbon Powder is electro-conductive with a low loading quality. It also has minimal reduction in electro-conductivity when mixed with other materials. As the chemical agent material, we used Sodium Dodecyl Benzene Sulphonate which is sensitive to water hardness and it is difficult to be oxidized. It also has properties like emulsility and dispersity which is useful in chemical solutions for electrochemical cells. [38]

3.5.5 Ion Selective Membrane

The membrane prevents the transportation of electrons between the half cells and only allow the transport of ions to maintain charge equilibrium between the half cells. The membrane is durable which is essential since a flow battery has a long cycle life. It is also conductive which helps the movement of ions through the membrane.

3.5.6 Case

As the casing material, we used Polypropylene. Polypropylene is a thermoplastic polymer which does not undergo chemical change when they are heated and it can be molded. It is tough, flexible, has a good resistance to fatigue, and has low conductivity. [39]

3.5.7 Pipe

Pipes together with the connectors allow the flow of the electrolyte mixture from the storage tank to the electrochemical cell and has a high resistance to corrosion. The selection of the tubing material is very important as the leaks, cracks, and ruptures can cause the battery system to fail.

3.6 Technical Specifications of Flow Batteries

The following sections presents technical specification of flow batteries including energy density, current density, and power density. Those quantities show the basic performance measurements of the battery.

3.6.1 Energy Density

Energy density is a characteristic of the battery chemistry and it is determined by the solubility of active materials in the electrolyte mixture. Its unit is Watt-hour/Liter as it is the energy that can be derived per unit volume of the cell. [33] It determines the storage tank size required to achieve a given energy capacity. In many applications, the availability of space for placing a storage tank must be minimized, and thus energy density must be as high as possible.

3.6.2 Current Density

Current density is the available current per surface area of the electrode where chemical reactions take place. The steady flow of electrolyte mixtures enables more reactions to take place at the surface of the electrode, therefore increasing the reactions per unit area, resulting in high current densities. [40]

3.6.3 Power Density

Power density is the maximum available power that can be derived per unit volume and its unit is Watt/Liter. It is a characteristic of the battery chemistry and it determines the electrochemical cell size required to achieve a given performance output. For a given cell chemistry, increasing the surface area of the electrodes can increase the cell's current at a given current density, thus delivers more power. [33]

4.0 Design

The battery is designed for testing, so the dimensions of plate, channels, etc. were chosen so that it is manufacturable. Large scale applications will require bigger plates, and studies need to be done in order to determine the optimal channel sizes, distance between channels, etc.

4.1 Chanel configurations

The three most common chanel configurations for cell design are serpentine, parallel, and inter-digitated flow. [27] These chanel configuration designs are shown in figure 11. Each has advantages and disadvantages. The group decided to follow the parallel flow channel design since it has some desired advatages and is manufacturable. One important advantage of this design is that the pressure drop in the parallel flow design is low. Hence it may eliminate potential leaking and reduce the power needed to pump the suspension. Also, this design works for very large plates and high current density operations, which is the main application of flow batteries. The disadvantages of this design are that an obstruction in one channel may cause flow redistribution in the remaining channels and the first few channels may have a greater amount of suspension compared to the last few channels. [28]

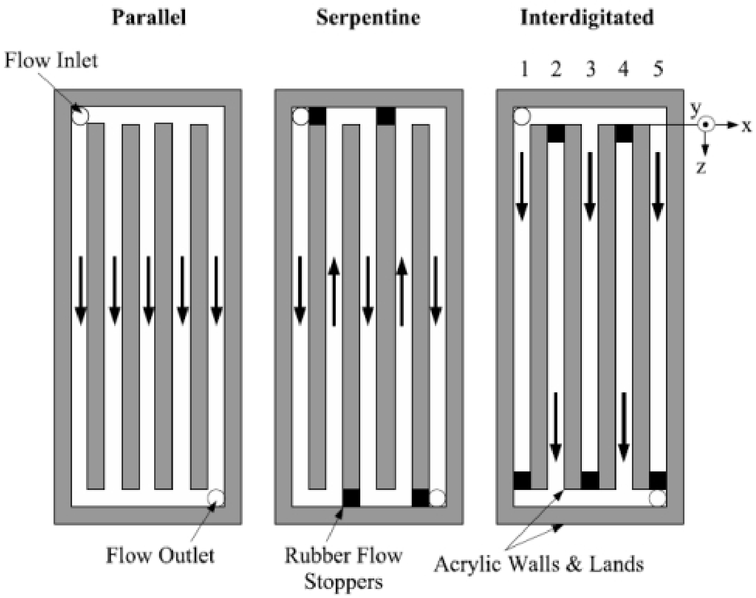

Figure 11 Three most common flow field design

4.2 Plate Dimensions

Figure 12 shows our plate design in SolidWorks. The plate has 10 channels and there are two deep holes to connect and provide suspension to the channels. The suspension will go into the first hole then flow through all of the channels and then exit at the second hole. The outer region of the plate is lowered (which contains channels) so that a rubber ring can be placed. The role of the rubber ring is to prevent leaking.

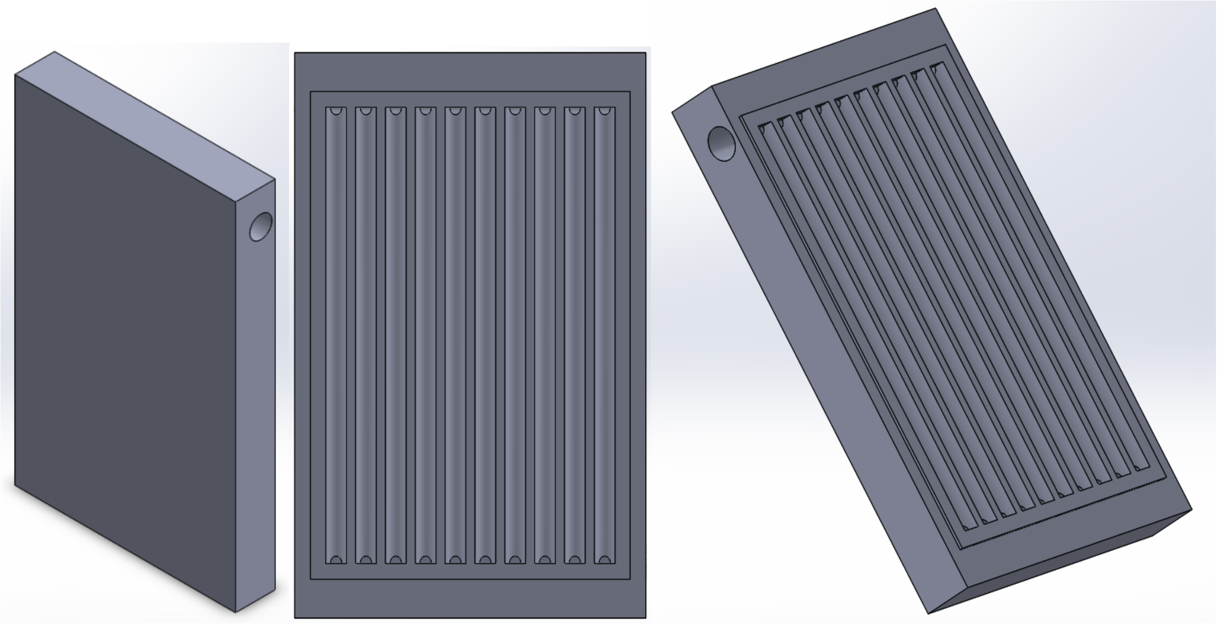

Figure 12: Plate design in SolidWorks, from the left Back, Front, and 3D

Our plate dimension is 2x3.22x0.38 inches. There are 10 semicircle channels; each having a 0.06 inch diameter and a 2.6 inch length. There are two holes used to connect these channels, each having a 0.20 inch diameter and a 1.85 inch depth. The outer region is 0.02 inches lower than the rest of the plate. A detailed two-dimension drawing showing the dimension of the plate is shown in Figures 13.

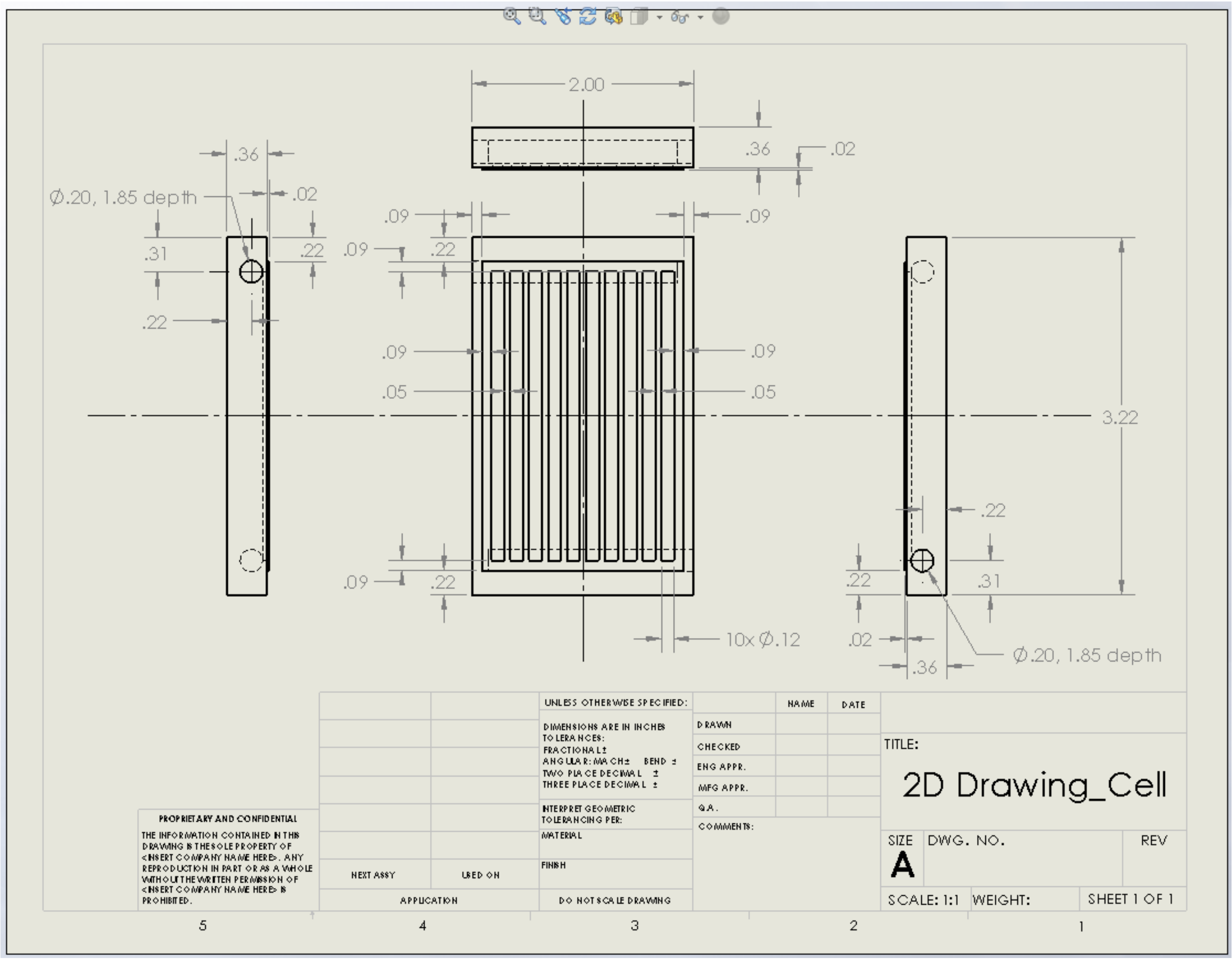

Figure 13: A 2D Draw showing detail dimension of the plate

5.0 Manufacturing Methodology

Proper machining of our prototype is a crucial aspect to this project. With only having one set of Nickel and Copper plates, any mistakes during this process was detrimental to a successful and efficient prototype. The process of programming and machining our design was a long and tedious process but extremely imperative to be completed in a timely matter and properly.

5.1 Programming with ESPRIT

In order to begin machining the Nickel and Copper plates after modeling our final design in SolidWorks, it was necessary to transfer the design to ESPRIT (a powerful computer aided manufacturing software). The software would generate the appropriate G-code needed to properly machine our parts using a 3-axis CNC Haas Minimill.

Although ESPRIT is an extremely powerful program, at times it can be finicky and complicated to use. The software first requires the user to import their CAD file in order to have a base of the solid that is to be recreated with the same geometry that was modeled. If the user is importing a CAD file into an existing template, it is extremely important to "merge" the model in order to properly program that part. As a precautionary measure, before the user continues to program the geometry, it's recommended that the machine set up is modified to ensure that Dogleg Rapid is "on". A rapid move is when the machine tool moves between two points but does not actually remove any material from the part. Having Dogleg Rapid on allows the machine to make a rapid movement in a non-linear fashion (so not in a straight line between two points). The machine would move the tool in each axis at full speed until it reaches is final position. In the end, this allows for a shorter machine run-time and smoother accelerations/decelerations. Also, the user should set up the software's simulation settings by turning on collision detection. This feature is useful since it can tell the user during simulation if the machine will crash. It is good practice to have this on early since the user may constantly simulate their operations while working on the program. Lastly, in order to see the part being machined in the simulation, the user must create a basic solid that will represent the shape of the part to be machined (as opposed to the final shape of the design). This is simply done by selecting a shape (a block in our case) and submitting the dimensions.

Since the model created in SolidWorks already has the appropriate dimensions and shape, the only fix that needs to be made with its geometry is its position and orientation on the axis. This is a crucial part in the programming since it determines how the stock metal should be fixed in the machine; as it turns out, the features that are to be machined on the part determine how the stock should be fixed, thus, how it should be oriented in ESPRIT. For example, the features in our part include the ten channels on the top surface, a lowered edge also on the top surface for a rubber ring (that will keep the membrane in place) and two holes that connect the channels and allows the suspension to flow through. The channels and the lowered edge require an orientation such that these features are pointing in the same direction as the positive z-axis (+z), or parallel to the x- and y-axis. However, since the holes are on the sides of the plate, a second ESPRIT program must be made in order to have these features point in the same direction as the positive z-axis since this 3-axis machine is only capable of drilling in this direction. Nevertheless, since the two holes are mirrored from each other and have the same dimensions, the same program can be used to drill each feature.

Even though having two different ESPRIT files satisfies the needs of machining the features designed in SolidWorks, it doesn’t take into account the differences between the dimensions nor the shape of the design and the stock. The Nickel and Copper plate we acquired were not the same dimensions, nor were they the proper dimensions we needed for our design. Also, the Copper plate had some minor deformations, whereas the Nickel plate had a significant arc to its shape. In order to accommodate the improper dimensions for both the Copper and Nickel plate, we decided to have separate programs for the two parts. In order to machine the lateral sides of the two parts to their proper dimensions, a contouring operation was included in the same program we used to machine the channel and lowered edge features. A new program had to be created to properly dimension the top and bottom faces of the plates. The same program was used to machine these two faces and were the only dimensions adjusted between the two parts. So in total, we had 6 ESPRIT programs: 2 for the channels, lowered edge, and lateral contouring features (one program for each material), 2 for the holes, and 2 for the top and bottom face dimensioning. Finally, with these 6 programs, setting the orientation of the solids is quite simple; it involves rotating the solid about a certain point on either axes until the proper face is pointed towards the positive z-direction. Also, it's convenient to have the top of the surface (surface perpendicular to the z-direction) at z=0. When probing the tools and the stock within the machine (mentioned later), the tip of the tool assumes it comes into contact with the stock at z=0. If the program doesn't have this default, it's easy to set an off-set to make the adjustments but requires more steps on the CNC machine. Once the geometry is complete, the next step is to create the tools required to make the correct cuts in ESPRIT.

Creating tools in ESPRIT is quick and easy; however, if any inputted information is incorrect, it's possible to break the tool and/or the part you are machining. For our plates, we used the following tools: a 3/8 Non-Ferrous End Mill, a 3/8 Ferrous End Mill, 1/8 Non-Ferrous Ball End Mill, a 1/8 Ferrous Ball End Mill, a Steel/Cobalt #7 Drill, and a carbide coated #7 drill. The difference between a Ferrous and a Non-Ferrous tool is the simple fact that ferrous tools contain iron, while Non-Ferrous tools do not. Also, Ferrous tools have a higher strength compared to Non-Ferrous tools and possess magnetic attraction, while Non-Ferrous tools have higher melting point and are resistant to corrosion. In our case, we used the ferrous tools on the Nickel plate and the Non-Ferrous tools on the Copper plate. Copper and Nickel aren't machined too often so working with these metals and finding appropriate values was an interesting challenge. We learned that Copper work hardens pretty dramatically, so we were advised to take fairly deep cuts, and use aggressive feed rates and sharp tools. Work hardening is the process in which a metal's strength increases due to plastic deformation and because of dislocation movements and generations within the crystal structure. Each tool had specific values that had to be submitted into ESPRIT in order to acquire the desired cuts. Some of these values include, but not limited to, the axis orientation, the shank diameter, tool diameter and length, shank diameter, tip angle, flutes, threads, and two of the most important values are the feed and speed rates. The "cutting speed" is the relative velocity between the cutting tool and the surface of the work piece, whereas the feed rate is the relative velocity at which the cutter is advanced along the work piece. So basically in a mill, the cutting speed is tangential to the outer diameter of the cutting tool and usually measured in surface feet per minute (sfm), and the feed rate is how fast the tool moves along the work piece per revolution, which can be measured in inch per tooth. If the wrong values are entered into ESPRIT for feeds and speeds, the tool and/or the work piece can be damaged. A company called Kennametal provide various feeds and speeds associated with certain types and sizes of tools, and our group references their information for our machining. Each tool has a different feed and speed rate, since these values are determined by the size of the tool and the material in which it is cutting. The 3/8 End Mills were used to cut the lowered edge and the dimensioning of the faces. The 1/8 Ball End Mills were used to cut the channels, and the #7 drills were used to cut the holes.

Although at this point the solid that holds our design has been imported and oriented in ESPRIT, it's still essential to program the paths at which the machine tools should follow and this is technically still creating the geometry, but specifically so that the machine can recognize where all the surfaces are on the solid. The first thing to do is to "smash" the solid, which basically takes the body of the part and creates a geometry on it within a given tolerance (0.0005 inches in our case). However, another procedure must be done in order to identify the body. Now that the geometry is available (due to smashing), we then have to create a "part profile" of the body (within the same tolerance of 0.0005) which will allow ESPRIT to create (or trace) the features the work piece has. In summary, we can now draw the specific paths we'd like the tools to follow once we create the features on the part. The way this is down is by creating "chains", which are basically curves that trace the shape of the desired features; for example, features were created for the channels and the lowered edge. It is basically another process of distinguishing the exact shape of the solid. Since the dimensioning isn't exactly a functional feature of the solid, nor was it designed in SolidWorks, we had to create a manual chain around the solid in order to program the machine where the tool should start cutting and how deep it should go (although the depth of cut is programmed during the operations step, which will be mentioned further on). An easy way to create this chain (since the curve won't actually be on the solid) is to create four points around the solid and connecting them with a chain. Normally a chain is defined as a boundary through which the tool is not allowed to pass; we can bypass this by making the chain "open", which changes the behavior of the chain, making it so the tool is now allowed to pass through the chain and out to a certain specified off-set (our desired dimensions in this case). An aspect that we had to consider is how deep we can cut into the lateral sides of the part. Since the part will be placed on a fixture, some of the bottom portion of the metal will be enclosed and unreachable. So instead of contouring the sides all the way through, we did half on one side, then flipped the part upside down, and repeated that portion of the operation. Similarly, this was done with the drilling operations for the holes.

Creating a feature for a hole works somewhat differently, but is simpler and less tedious than the other features. The user just has to create a PTOP (point to point) feature where a hole will be drilled. This basically determines the location of the center of the hole and its diameter. It is important to verify that the location of the PTOP point is truly at the center of the hole, and that it is leveled with the surface you wish to start from. This will guarantee that the location of the hole and how deep the tool drills is correct, and with that, all the features were created. This allows the user to create the specific operations needed to machine the part.

ESPRIT has several different options for creating operations such as contouring, drilling, tapping, pocketing, etc. Each operation has specific and different details and variables that need to be submitted in order for the procedure to work desirably. Some of these parameters include the mode of entry, whether an operation should follow a zig-zag pattern or a spiral, starting depth, total depth, incremental depth, and feeds and speeds just to name a few. However, one of the most important parameter that each operation includes is the selection of the pre-created tool associated with said operation. As mentioned before, a contouring operation was used for the lateral dimensioning, a facing operation was used for the top and bottom surface dimensioning, contouring was also used for the lowered edge and a pocket operation was used for the channels.

Before a G-code can be generated and imported to a CNC machine, it is wise to run a simulation of the machining process to ensure that each operation are running smoothly and to make sure no collisions are detected (in fact, running the simulation after creating each operation to check for flaws would be a wise idea). If everything runs smoothly, the program is ready to be imported to a CNC machine.

5.2 Operating a HAAS Minimill

Operating the 3-axis HAAS Minimill can be exciting but also intimidating. Any negligence to the machine and its function can ultimately damage the part or the machine. Safety is also a concern and the users should always be fully aware of their surroundings. Also, Nickel and Copper are not machined too often so some of the speeds and feeds weren't listed on the Kennametal website so we had to use suggestions from lab monitors or call them directly. This made us especially aware and cautious of the machine and we were always ready to use the emergency stop function if we needed.

One of the first steps is to power up the machine and to reset the emergency stop and alarms. We can then send the machine to its home position. Before continuing, simulate the program in ESPRIT one last time to ensure no errors will occur. If all is set and clear, you can create the NC Code which will eventually be sent to the mini mill.

Now that the code is ready, the next step was to insert the tools we planned to use (recall that there are 6 programs, each using different tools) into a tool holder, which can be loaded into the machine. Once these tools are loaded, it's necessary to probe (or calibrate) each tool so that the machine is aware of each tool length. Similarly, we then had to tram our work piece into a vice, where it would sit on two parallels to stay leveled then probed to ensure that the machine is aware of where the plate is located and its corresponding dimension. Once everything has been probed, the user can upload the NC-code generated by ESPRIT into the CNC machine. Once the data has transferred, it is imperative to select the program we have loaded and simulate the operation yet again through the HAAS Machine, which will be our last chance to realize any mistakes that the program may have. After the simulation, there are only a few more modifications necessary to fulfill before we can run the machine. First, it's a good idea to reduce the rapid rate (rapid motion) to at least 5% (maximum of 25%). Lastly, the user must reset the memory from previous programs that may be on the machine and send the machine to its home position. The machine is now ready to run so the first thing you must check is to see if the coolant is functioning. Cutting coolant is extremely useful because it keeps the cutting material at a reasonable temperature, maximizes tool life, and prevents rust on machine parts and cutters. Finally, once it is confirmed that the coolant is on and working, it is wise to stop the feed as the tool becomes close to work piece. At this point, verify that the “distance to go” (distance the tool has to travel before it reaches the work piece) seems sound. If the coordinates look okay, let the machine cycle start and closely watch as the tools remove materials. If for any reason, something seems wrong (see sparks) use the emergency stop to bring the machine to a halt and access the problem.

This is the process we took to machine our plates and if it were necessary, we would use a file to sand off any remedies that may have still been attached to the part.

6.0 Testing Methodology

Conventional flow battery usually includes electrolyte mixtures circulated through a charge cell for producing an electrochemical reaction and electrical generation via ion transfer and by the movement of electrons. However, the charge density of conventional electrolyte mixtures tend to be relatively weak per unit volume of electrolyte and such electrolyte mixtures become saturated and precipitate out, limiting the quantity of charge material that may be dissolved. Therefore, large volumes of electrolyte mixtures must be employed and circulated to generate a useful energy component in the form of electric charge. In order to overcome the shortcomings of conventional solution-based flow batteries, we have used a charge suspension having a high charge density for generating substantial electrical energy from a relatively manageable volume of charge material via anodic (anode) and cathodic (cathode) suspensions.

6.1 Preparing the Chemical Suspensions

To be able to test the performance of our flow battery, we have prepared electrochemical suspensions to circulate them through our cell. This way, we have obtained performance characteristics of our prototype including energy density, power density, and efficiency. As half reactions occur inside the cell of our flow battery, it is required to have both anode and cathode electrolyte mixtures, prepared separately.

Due to the safety procedures, we have used chemical resistant gloves and facemask when interacting with chemicals. As a first step, by using an electronic balance, we have weighed carbon powder and SDBS and we have obtained 0.6g of carbon powder and 0.6g of SDBS. We handled the chemicals with a ladle which was cleaned with distilled water every time we changed the chemicals we were using. By using two separate grinders, we have lowered the size of the carbon and SDBS particles in order to increase their surface area, while maintaining higher solubility. Then, the grinded SDBS and carbon powder were added to a glass veil. The chemical agent and the carbon powder can be considered together as a stabilizing agent, which is used to stabilize the solution and avoid settling. In addition, the carbon powder increases the electrical conductivity of the electrode. The stabilizing agent, discussed above, facilitates the formation of a suspension having a greater charge density than conventional solutions, which are prone to precipitate out charge materials when the concentration becomes too high.

Then 12mol/L Potassium Hydroxide (KOH) electrolyte was mixed with the stabilizing agent inside the glass veil by using the electronic balance to weigh the KOH with the help of the pipette (chemical dropper). After that, the glass veil was placed into the sonic vibrator for 1 hour to agitate and homogenize the solution. The procedures discussed above provide the first three components of the electrolyte mixture that can be used in a half cell. Those procedures are similar for both anode and cathode electrolyte mixtures, so it is repeated one more time to have another glass veil which includes similar amounts of carbon powder, SDBS, and Potassium Hydroxide to obtain the first three components of the electrolyte mixture that can be used in the second half cell.

After that, we moved into the process of adding the charging materials into the glass veils we have prepared before. In our flow battery, Zinc Oxide (ZnO) is employed as the anodic (anode) charge material and Nickel Hydroxide ($Ni(OH)_2$) is employed as the cathodic (cathode) charge material. The anodic and cathodic charge materials are prepared using a mixer for a predetermined time before adding into the glass veil. First of all, 4g of cathodic charge material, Nickel Hydroxide ($Ni(OH)_2$) was weighed by using the balance and then added into the glass veil. $Ni(OH)_2$ powder coated with Cobalt Oxide Hydroxide (CoOOH) was used since CoOOH has higher electronic conductivity. To improve further conductivity of the suspension, 4g of Nickel powder was added into the glass veil. The Nickel powder that we used was 99% pure Nickel. As a result, we obtained a substantial 17% Nickel Hydroxide suspension which can be stated as a cathode electrolyte mixture. Also, 4g of anode charge material (Zinc

Oxide) was weighed by the balance and added into the second glass veil to obtain a substantial 23% Zinc Oxide suspension which can be stated as anode electrolyte mixture. Then, we homogenized all of the solution by agitating for another hour in the sonic vibrator to further decrease the particle size of the suspension and to increase the energy density of the suspension. As a final step, we stirred the electrolyte mixtures by using the grinder for one more hour to make sure all particles inside the electrolyte mixture is evenly distributed and we don't have any large pieces of particles that is not mixed inside the mixture; as a result, we obtained stable electrolyte mixtures. The disclosed approach combines the advantages of high energy density suspension and Ni/Zn chemistry and offers a distinguishable design of flow batteries with high power densities at a low cost.

Figure 14: Electrolyte mixtures prepared. Upper image shows anode electrolyte mixture and the lower image shows cathode electrolyte mixture.

6.2 Assembling the Battery

To be able to circulate the suspension that we have prepared to flow through the electrochemical cell, it is very important to set our prototype carefully to make sure every material is placed in their correct positions. This way, it is possible to prevent the leakage of the chemical suspensions during the charging and discharging process, prevent wasting the chemical suspension, and also obtain accurate performance metrics. For those reasons, we have used Polypropylene casing which is plastic and has low conductivity so it can not affect the movement of electrons during the operation of the battery. In addition, we used metal latches to keep the casing in the desired position and it keeps the battery system tight. Before inserting the Nickel and Copper electrode between the casing materials, we connected the tubing material to the connectors on both side of the electrodes. Those connectors connect the holes of the electrodes to the tubing material. Apart from that, we polished the electrodes to make sure they have very high resistance to each other. The polishing was also necessary since a rough surface would actually pierce small holes into the membrane. Between the casing materials and the Nickel and Copper electrodes, a Copper current collector was attached to both sides of the battery in our system. Furthermore, three layers of ion selective membranes and two layers of rubber rings were placed between the Nickel and Copper charge plates. The rubber rings used only surrounded the 10 channels of the electrodes so it would not prevent the ion selective membranes to contact the electrolyte mixtures and the electrodes. The ion selective membrane separates the two half cells from each other and only allow the exchange of ions between the electrolyte mixtures. The rubber ring prevents the leakage of the chemical suspension and helps keep the layers of the ion selective membranes in their appropriate positions. The battery configuration can be seen in figure 15.

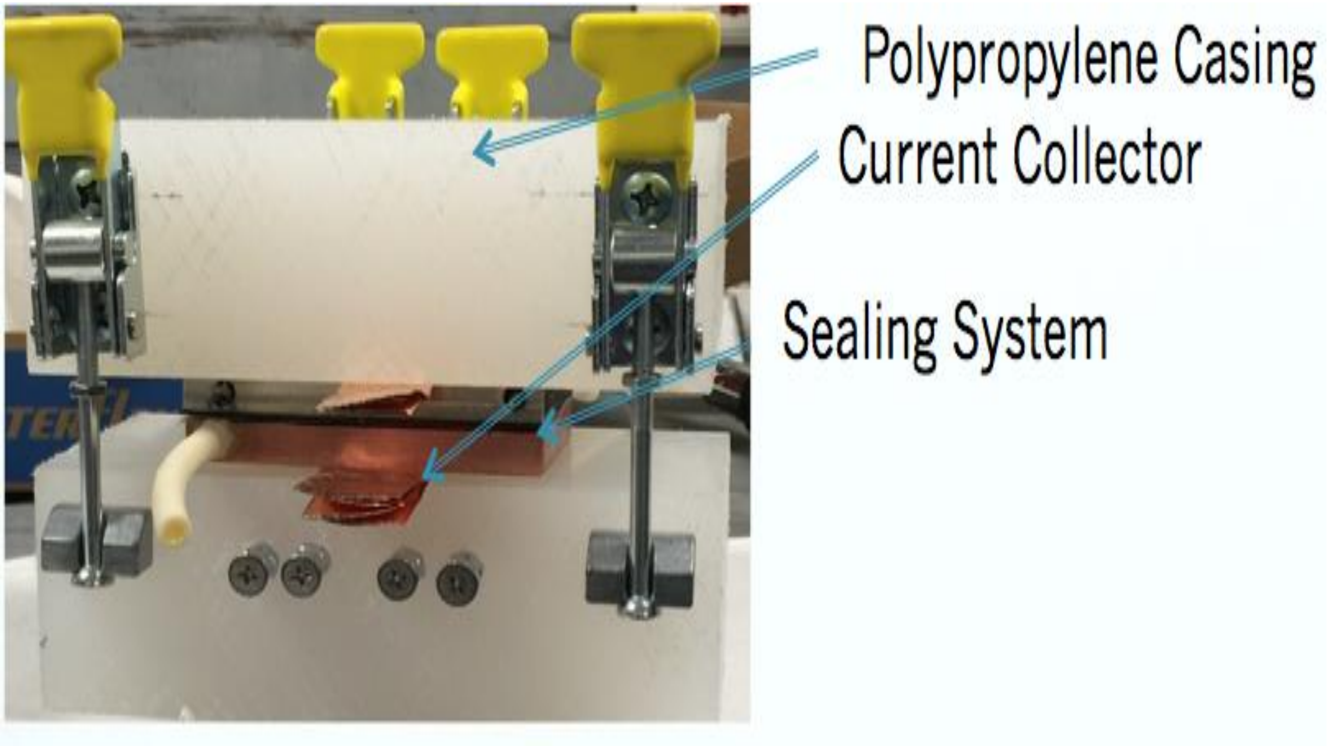

Figure 15: Materials used in our prototype.

6.3 Charging and Discharging Process of the Battery

After we finished assembling our flow battery prototype, we started filling the electrolyte mixtures into the electrodes by using a syringe. First, we filled two syringes with the cathode electrolyte mixture and anode electrolyte mixture, respectively. Following that, we inserted the first syringe (which contains cathode electrolyte mixture) into the tubing that is connected to the Nickel electrode. Then, we transferred the cathode electrolyte mixture from the syringe into the Nickel electrode. After that, we inserted the second syringe (which contains anode electrolyte mixture) into the tubing that is connected to the Copper electrode. Then, we transferred the anode electrolyte mixture from the syringe into the Copper electrode. As a result, both electrolyte mixtures flowed through the channels of the electrodes and then moved to the exit hole of the charge plate that is connected to same tubing material on the other side of the electrode. The following figure shows this process.

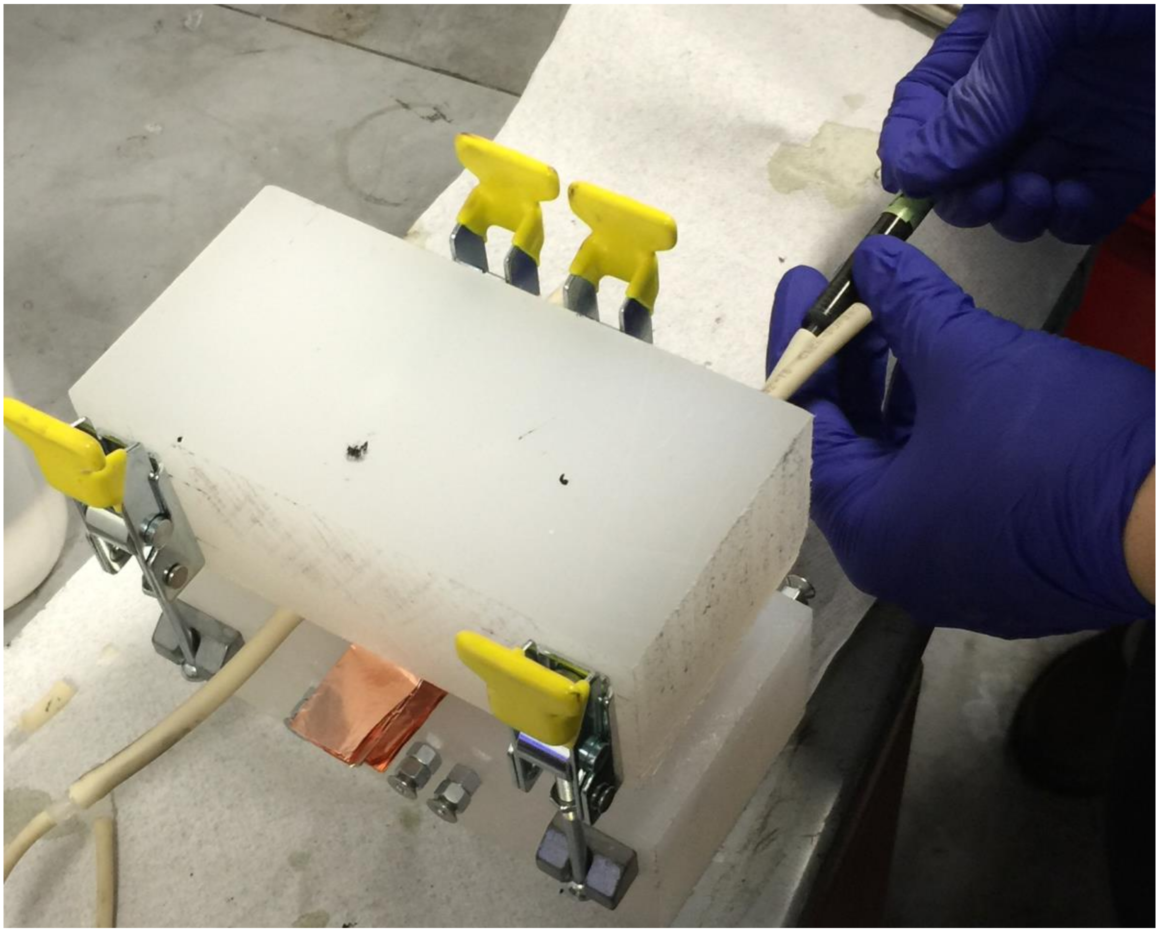

Figure 16: Filling the tube with the cathode electrolyte mixture.

In addition, we closed the tubing that is connected to the inlet hole of the electrode with the tubing that is connected to the outlet hole of the electrode, for both Nickel and Copper electrodes, to make sure the electrochemical system is sealed and all chemical suspensions will stay inside the electrodes during the charging and discharging process. After that, by connecting crocodile clips to the Copper current collector (which was attached to both Nickel and Copper plates) we set up an external circuit that connects our flow battery to the computer and to the electrochemical channel analyzer.

For the charging process of our battery, certain current and voltage values were set by considering the charge capacity of the battery in order to charge the battery in a specified time frame. We then discharged our battery in said time by again determining the specific current and voltage values. For the next cycle, we have changed the applied current to observe the differences in the voltage and current characteristics of the battery during the charging and discharging process. As a result, the charging and discharging cycle time varied. We conducted testing experiments of our battery three times to make sure we obtained reliable performance results for our prototype. In each testing experiment, we charged and discharged our battery 10 times which means we have obtained 10 cycles of performance characteristics.

7.0 Improvements on Design, Manufacturing, and Testing

We were able to determine what was needed to be improved with our initial design after attempting to machine the fuel cells and after the testing. Machining the channels and lowered edges of the Copper and Nickel plates were both successful; however, machining the inlet and outlet holes for both plates proved to be difficult. We first drilled an inlet hole on the copper plate using a pecking operation, which then showed us a flaw in our design. The hole was too close to the top surface of the plate, thus was slightly exposed on the same groove as the lowered edge. This error would allow the suspension to leak out of the channels. We used a #7 drill for this operation and wanted to thread the holes afterward in order to insert a pipe adapter, which was not possible now. The location of this hole is crucial because it actually exposes small holes where the channels are, which allow the suspension to flow through each channel. With that, even a new design with the hole located further away from the surface would not work since these holes on the channels would not be exposed. In the end, we were able to fix this issue by using an epoxy to connect the pipe adapter. Since the adapter was threaded, we used a knife to carve the threads so it could fit soundly in the inlet hole, which can be seen in the following figure.

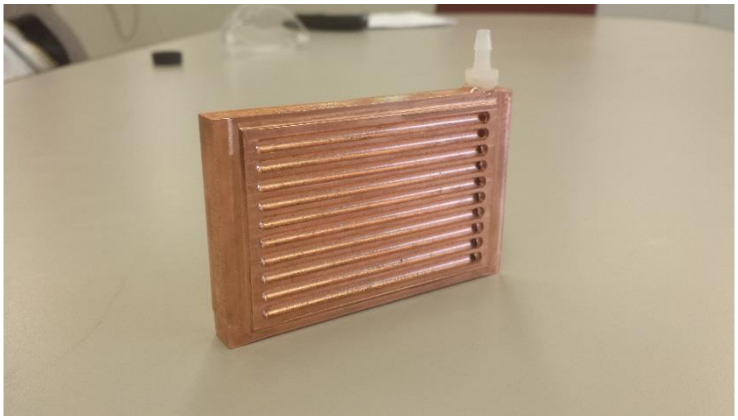

Figure 17: Epoxy sealed pipe adapter

We connected the pipe adapter using this method for both holes for the Copper and Nickel plates. The design may be improved by neglecting the lowered edge. This feature is not crucial to the plate, and having the extra room seems to be far more important. The edge allows a rubber ring to fit slightly better to hold the membrane in place, but it not completely necessary.

Machining the holes for the Nickel plate was a much more challenging process. Nickel has a material property that makes it difficult to machine easily: it work-hardens, meaning as the material is introduced to stresses, it increases in strengths and becomes harder. It was suggested by the lab monitors that a carbide coated drill bit should be used to machine the holes; however, these tools are not available in the machine shop. With that we were given two options: order the proper drill bit ourselves, or modify the feeds and speeds and use a Steel or Cobalt drill bit, which are available in the shop. Being confident that the Steel #7 drill would work fine, we went ahead and used the already available tool. Unfortunately, the tool broke during the drilling operation, thus resulting in a few channels becoming non-functional. In order to salvage what we had, we decided to order the carbide coated drill bit and use the other side of the plate to drill the hole. This would mean only 6 of the channels would be functional. We machined the hole again on the other side, but to our surprise, the drill bit broke again. After further research and even contacting Kennametal and speaking to technical support, we learned that our feeds and speeds were slightly too high, but more importantly, we learned that we were using the wrong drilling operation for Nickel. As mentioned before, Nickel work-hardens so using a pecking operation (a drilling operation where the drill bit will drill the hole at depth similar to its diameter multiple times, rather than drilling a hole all the way through) would make it difficult to machine since the material becomes stronger each time the drill bit re-enters the hole. The following figure shows the results of the operation.

Figure 18: Nickel plate with broken drill bits

Having this new information, we were able to successfully drill two holes on the opposite side of the plate. Unfortunately, only 4 of the 10 channels were functional, meaning we will have lower numbers for our results after testing. If time permitted, we would have acquired a new Nickel plate and machine the plate again, taking into account the information we've received machining it the first time and using the improved ESPRIT program (with modified operations, feeds and speeds).

Preparing the chemical solutions of the battery takes a lot of time; even preparing a small amount of solution was long and tedious. In order to prepare the solutions faster and obtain considerably high amounts of suspension, a Ball Milling apparatus can be used to stir the solution, which would also further decrease the size of particles inside the solution. In addition, in order to achieve higher energy densities and increase the stability of the suspension, polymers and dispersants like polyethylene glycol can be added into the solution. Polymers would support the stabilizing agent to maintain the charge material in the chemical suspension and dispersants would enhance the even mixing of small particles within the solution.

8.0 Discussion of Results

Nickel and Zinc suspensions have high energy densities (162.35 Wh/L and 422.24 Wh/L, respectively); section 7.1 includes theoretical calculations for high energy density Nickel and Zinc suspensions. Section 7.2 includes battery experiment results. A discussion of the results and recommendations for future projects are presented in section 7.3.

8.1 Theoretical Performance

Table 4 shows the first suspension composition (Nickel suspension) and table 5 shows the second suspension composition (Zinc suspension). The weight percent (w%) and volume percent (v%) of each component were calculated from the mass of each composition we used in our experiment. The suspensions densities were also calculated based on the density of each component.

Table 3: Suspension Composition (Nickel suspension)

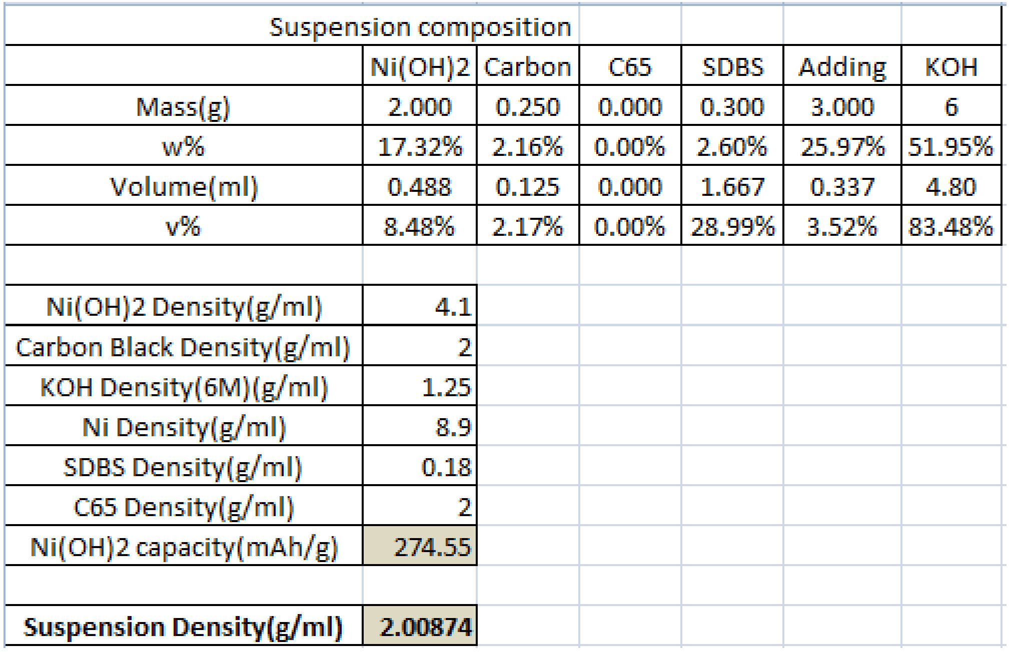

Suspension composition						
	Ni(OH)2	Carbon	C65	SDBS	Adding	KOH
Mass(g)	2.000	0.250	0.000	0.300	3.000	6
w%	17.32%	2.16%	0.00%	2.60%	25.97%	51.95%
Volume(ml)	0.488	0.125	0.000	1.667	0.337	4.80
v%	8.48%	2.17%	0.00%	28.99%	3.52%	83.48%
Ni(OH)2 Density(g/ml)	4.1					
Carbon Black Density(g/ml)	2					
KOH Density(6M)(g/ml)	1.25					
Ni Density(g/ml)	8.9					
SDBS Density(g/ml)	0.18					
C65 Density(g/ml)	2					
Ni(OH)2 capacity(mAh/g)	274.55					
Suspension Density(g/ml)	**2.00874**					

Capacity and Energy Density for the Nickel suspension calculations are as followed:

$$Specific\ Capacity\ Density\ (mAh/g){:}\ Ni(OH)_2\ capacity\ (mAh/g)\ *\ weight\ percent\ of\ Ni(OH)_2$$

$$= 274.55(mAh/g) * 0.1732 = 47.54\ (mAh/g)$$

$$Capacity\ Density\ (mAh/ml){:}\ Specific\ Capacity\ Density\ (mAh/g)\ *\ Suspension\ Density\ (g/ml)$$

$$=\ 47.54\ (mAh/g)\ *2.00874(g/ml)\ =\ 95.5\ (mAh/ml)$$

$$Specific\ Energy\ Density\ (Wh/kg){:}\ Specific\ Capacity\ density\ (mAh/g)*Working\ Voltage$$

$$=\ 47.54\ (mAh/g)\ *1.7V\ =\ 80.82\ (Wh/kg)$$

$$Energy\ Density\ (Wh/L){:}\ Specific\ Energy\ Density\ (Wh/kg)\ *\ Suspension\ Density\ (g/ml)$$

$$=\ 80.82\ (Wh/kg)*2.00874(g/ml)\ =\ 162.35\ (Wh/L)$$

Table 4: Suspension Composition (Zinc suspension)

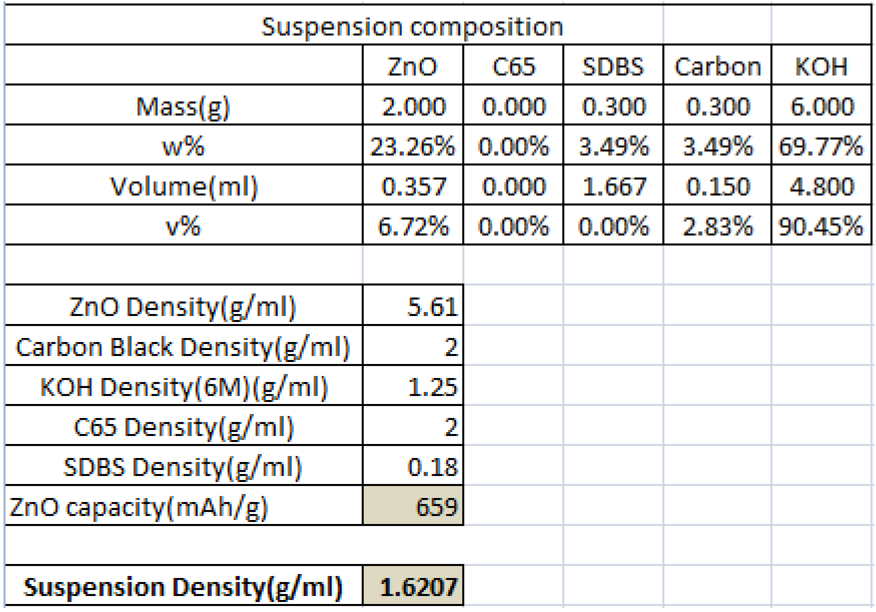

Suspension composition					
	ZnO	C65	SDBS	Carbon	KOH
Mass(g)	2.000	0.000	0.300	0.300	6.000
w%	23.26%	0.00%	3.49%	3.49%	69.77%
Volume(ml)	0.357	0.000	1.667	0.150	4.800
v%	6.72%	0.00%	0.00%	2.83%	90.45%
ZnO Density(g/ml)	5.61				
Carbon Black Density(g/ml)	2				
KOH Density(6M)(g/ml)	1.25				
C65 Density(g/ml)	2				
SDBS Density(g/ml)	0.18				
ZnO capacity(mAh/g)	659				
Suspension Density(g/ml)	**1.6207**				

Similar to the calculation for Nickel suspension, Capacity Density and Energy Density were determined for the Zinc suspension:

Specific Capacity Density (mAh/g):	153.26 (mAh/g)
Capacity Density (mAh/ml):	248.37 (mAh/mL)
Specific Energy Density (Wh/kg):	260.53 (Wh/kg)
Energy Density (Wh/L):	422.24 (Wh/L)

Based on our flow battery design, the total volume of the 10 channels is 2.422 ml. The capacity and specific energy of Ni and Zn suspensions were determined:

Nickel suspension

$$Capacity: 2.422\ (ml) * \ 95.5\ (mAh/ml)\ =\ 231.3\ (mAh)$$

$$Specific\ Energy: 231.3 (mAh) * 1.7 (V)\ =\ 293\ (mWh)$$

Zinc suspension

$$Capacity: 2.422\ (ml) * \ 248.37\ (mAh/ml)\ =\ 601.5\ (mAh)$$

$$Specific\ Energy: 601.5\ (Ah) * 1.7 (V)\ =\ 1023\ (mWh)$$

Our Flow Battery theoretical capacity is 231 mAh (this value is limited by the Nickel suspension capacity). The current and power density depends on charging and discharging times. Let us assume that the discharging time is 10 hours which is a typical discharging duration time for flow batteries. The battery capacity, current density and power density were determined as follows:

$$Battery\ capacity: 231.3\ (mAh) * \ 3.6\ \left(\frac{C}{mAh}\right)\ =\ 833\ (C)$$

$$Current: I\ =\ 833\ (C)/36000\ (s)\ =\ 0.02314\ (A)$$

$$Current\ density: J\ =\ 0.02314\ (A)/\ 0.003096768\ (m^2)\ =\ 7.472\ A/m^2$$

$$Power\ density: P\ =\ 1.7 (V) * 7.472 (A/m^2)\ =\ 12.7\ W/m^2$$

8.2 Experiment results

Figure 12 shows a graph of two cycles of testing. The battery received 0.01A of current for approximately 70,000 seconds (about 20 hours). This charging process brought the battery to about 1.3V. The graph then shows that the current was brought down to about 0.005A over a period of 35,000 seconds (about 10 hours). The voltage remained constant during this time. However, during the discharging process, the current should have remained at approximately -0.005A longer in order to completely discharge the battery. Since it remained at this current for about 15,000 seconds (about 4 hours) and only discharged about 8% of the stored capacity, we can predict the outcome of the actual discharging process. Further testing results can be seen in the appendix.

$$\text{Efficiency} = \frac{Discharge\ Capacity(A.seconds)}{Charge\ Capacity(A.seconds)} * 100\%$$

$$Capacity = Current * Time$$

$$Discharge\ Capacity = (0.01A * 70{,}000s) + (0.007 * 40{,}000s) = 980\ A.s$$

$$Charge\ Capacity = (0.005A * 15{,}000s) = 75\ A.s$$

$$Efficiency = \frac{75}{980} * 100\% = 7.7\%$$

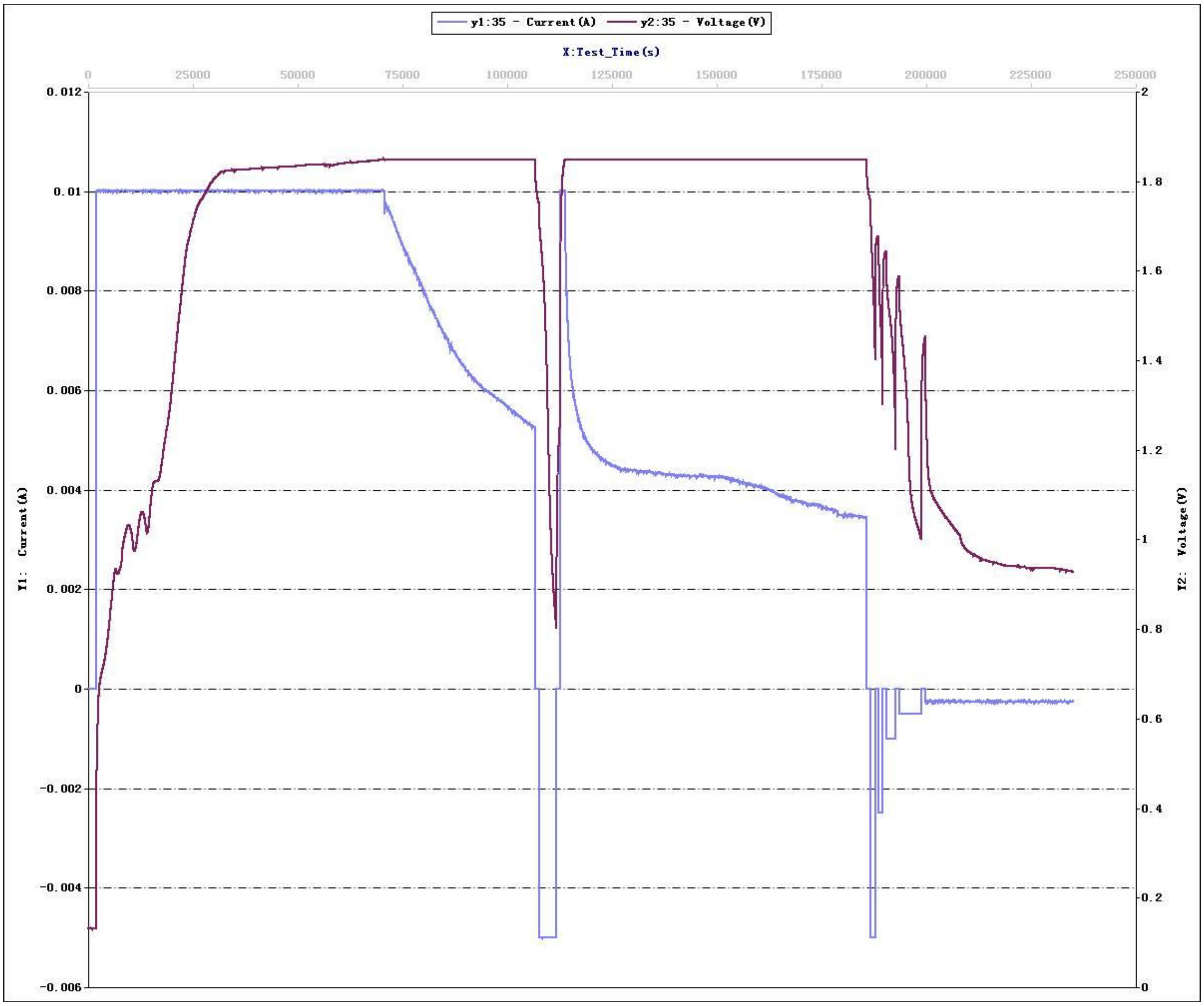

Figure 149: Charge and Discharge Characteristic of the Battery. Voltage and Current relationship against time is shown.

8.3 Discussion

There are differences between our battery experiment results and its theoretical performance. Flow batteries are expected to last several thousand cycles; however, our battery only lasted for five cycles. Furthermore, the battery efficiency is only 10% which did not meet our expectations. In fact, conventional flow batteries may reach an efficiency of 80%. Our battery has a theoretical capacity of 833 (C), but it can only store less than 100 (C).

The disparity between the theoretical performances and the actual results may be due to improper battery assembling during testing (the Copper and Nickel plates might not perfectly align), and contaminations in chemical materials. In addition, our battery was designed to have 10 channels;

however, it only has 4 channels in the Nickel plate and 6 channels in the Copper plate due to failures in the manufacturing process. As a result, the suspension filled all 6 channels in the Copper plate while only filling 4 channels in the Nickel plate; two channels in the Copper plate were filled with suspension but this amount of suspension would not create any electrical energy.

Future battery design projects may address above issues to improve battery efficiency and achieve higher power. The future project may also increase battery capability and power by including two external tanks and the number of cell stacks.

9.0 Future Applications and Considerations:

Nickel/Zinc flow batteries have high potential to be used for large-scale electric grid storage and high power applications such as transportation due to its high energy density, high power density, high safety, low cost, and high cycle life. Possible future applications of our flow battery include electricity storage for renewable energy sources like solar energy and wind energy. Along with that, hybrid and electric vehicles can be designed and fabricated to operate with our flow battery and an electric motor.

9.1 Electric/Hybrid Vehicles:

Insufficient performance and high cost of current storage systems prevent the world-wide use of electric cars. Our flow battery has the potential to offer high performance due to the combination of its multi-channeled electrode design and high solubility limit of the active materials in the solution used to be circulated between the charge plates. Also, materials used and the manufacturing processes demonstrate lower production costs when compared to current battery systems. There are more than one billion cars in the world and according to the U.S Environmental Protection Agency (EPA), 4.7 metric tons of carbon dioxide are emitted on average annually from a typical passenger vehicle. Therefore, by a radical transformation from internal combustion engine cars to electric cars, it is feasible to reduce oil dependency and lower carbon dioxide gases in the atmosphere that are emitted by conventional cars. By achieving high energy density and power density, we are willing to provide a better storage solution that would increase the performance of an electric car. The number of charge plates affects the power capacity of the battery, whereas the size of the tank used for storing chemicals determines the energy capacity of the battery. Therefore, arrangement of multiple cell stacks can provide desired power for an electric vehicle and the sufficient size of the tank results in high mile ranges with one discharging cycle. The size of the tank should be considered wisely since it is an imperative parameter which affects the weight of the car and the location of the tanks can affect the weight distribution of the car. Therefore, storage tanks need to be considered carefully so as not to lower the performance of the car. As flow batteries offer long cycle life, once it is installed into the vehicle, it does not need to be replaced every 5-10 years like Lithium-ion batteries do and the efficiency of the battery does not change with extensive use due to the replacement of the solution in the storage tank. However, as the solution in the storage tank needs to be changed once it is used, new stations will need to be built in order to pump the new solution into the tank and remove the wasted solution out of the system. Wasted solutions can be charged again using renewable energy sources by delivering the solution to the electricity generation grid. It is obvious that it will take several years to universalize this system and to compete with petroleum based vehicles.

9.2 Wind/Solar Energy Storage:

Energy derived from solar and wind sources shows discrepancy as the amount of electrical energy produced depends on the time of the day, season, and weather. Therefore, storage solutions present a high importance in order to ease the transient fluctuations. With the novel design of our Nickel/Zinc flow battery, we would like to bring a storage solution to both grid electricity and off-grid electricity production methods from solar and wind energy. Our flow battery can be manufactured with an affordable cost to offer a high energy conversion efficiency from chemical to electrical energy or vice versa and can be used for long periods without any alterations in efficiency.

Currently, expensive and limited life spanned storage systems force the electricity generated by renewable sources to be sent instantly into the grid to be used by the community without considering the actual electricity need of the community. This means that electricity is always available when the sun is shining and the wind is blowing. With the help of our flow battery, it is possible to store the extra electrical energy produced during the daylight as chemical energy and use that chemical energy during the night to generate electricity. This way, it is possible to distribute electrical energy according to the demand of the community and provide all day electricity from solar and wind energy. Our flow battery, like any rechargeable battery, is adaptable to both Concentrated Solar Power systems and Photovoltaic systems that are mainly used to generate electricity from solar energy by building large power stations. Along with that, Off-grid Photovoltaic systems that are used in residential buildings can store excess electricity produced by using our flow battery, whereas grid-tied systems in residential buildings can deliver the extra electricity to the transmission grid to meet shortfalls during peak demand periods.

Also, Onshore Wind Farms can be combined with our flow battery for storage during high-wind periods and when the production of energy is greater than consumption. In remote areas, small-scale off-grid wind power systems can be used together with our flow battery for household electricity generation. When we consider the finance of storage applications, our flow battery can increase the economic value of solar and wind energy since stored energy can be shifted to replace high cost generation during peak demand periods and the potential profit from that situation can offset the cost and any losses of storage. Overall, our flow battery demonstrates high potential to increase the reliability of current wind and solar energy production systems.

Calculations for a wind turbine energy storage using a flow battery are shown below:

Assume that a wind turbine has 25% capacity factor, a 1.5-MW turbine would produce 9 MWh:

$$1.5\,MW \times 24\,hours \times 25\% = 9\,MWh\ (in\ a\ day)$$

Also if we assume that the battery only needs to store half of the total wind turbine energy output (load balancing), the energy that the battery needs to store is 4.5 MWh. Our battery Specific Energy is 0.293 Wh (in theory) which means that we need at least 15 million stacks:

$$4.5 * 10^6\,Wh/0.293\,Wh = 15\,million\ stacks$$

Our battery is only about 10 percent efficient which means that we need far more stacks, which is not practical. In fact, our battery design is for testing; it does not even have external tanks. The number of stacks can be reduced if we increase the channels' dimension and the number of channels. More importantly, we can increase the energy capacity if we include tanks to contain more suspension.

The Nickel suspension’s energy density is 162.35 (Wh/L). The amount of suspension needed to store energy from the above wind turbine (12 hours operation) is $40*10^3$ L (assume that the battery can achieve 70% efficiency):

$$(1/0.7) * 4.5 * 106Wh/162.35\ (Wh/L)\ =\ 40 * 10^3\ L$$

A commercial flow battery needs to have around 40 cubic meters of Nickel suspension to store enough energy for a 1.5 MW wind turbine in a period of 12 hours. This large amount of suspension can be stored in an external tank. The bipolar plate design for this massive battery system needs to have the optimal channel size and number of stacks in order to increase efficiency.

References

[1] "BP." *Energy Outlook 2035 Shows Global Energy Demand Growth Slowing, Despite Increases Driven by Emerging Economies*. 15 Jan. 2014. Web. 10 Mar. 2015. <http://www.bp.com/en/global/corporate/press/press-releases/energy-outlook-2035.html>.

[2] "Pumped Hydroelectric Storage." *Energy Storage*. Web. 10 Mar. 2015. <http://energystorage.org/energy-storage/technologies/pumped-hydroelectric-storage>.

[3] "Pumped Hydroelectric Storage." *Clean Balance Power*. Web. 10 Mar. 2015. <http://www.cleanbalancepower.com/about-pumped-storage.html>.

[4] Dunlap, Richard. *Sustainable Energy*. SI ed. Timothy Anderson, 2014. 472. Print.

[5] "Solution to High Energy Costs Could Lie Underground." *Sandia*. 30 June 2008. Web. 10 Mar. 2015. <https://share.sandia.gov/news/resources/releases/2008/caes.html>.

[6] Dunlap, Richard. *Sustainable Energy*. SI ed. Timothy Anderson, 2014. 478. Print.

[7] "Flywheel Energy Storage System (FESS)." *Energy Storage Demo*. Web. 10 Mar. 2015. <http://energystoragedemo.epri.com/cec/fess/fess.asp>.

[8] Dunlap, Richard. *Sustainable Energy*. SI ed. Timothy Anderson, 2014. 483. Print.

[9] "Superconducting Magnetic Energy Storage (SMES)." *Energy Storage Sense*. Web. 10 Mar. 2015. <http://energystoragesense.com/superconducting-magnetic-energy-storage-smes/>.

[10] Dunlap, Richard. *Sustainable Energy*. SI ed. Timothy Anderson, 2014. 487. Print.

[11] Dunlap, Richard. *Sustainable Energy*. SI ed. Timothy Anderson, 2014. 488. Print.

[12] *Wikimedia.* Web. 10 Mar. 2015. <http://commons.wikimedia.org/wiki/File:Batteries_comparison_4,5_D_C_AA_AAA_AAAA_A23_9V_CR2032_LR44_matchstick-1.jpeg>

[13] "Flow Batteries." *Tantaline*. Web. 10 Mar. 2015. <http://www.tantaline.com/Flow-Batteries-568.aspx>.

[14] Boer, Petra, and Jillis Raadschelders. "Flow Batteries." *Leonardo Energy* (2007): 6. Print.

[15] Boer, Petra, and Jillis Raadschelders. "Flow Batteries." *Leonardo Energy* (2007): 5. Print.

[16] Boer, Petra, and Jillis Raadschelders. "Flow Batteries." *Leonardo Energy* (2007): 7. Print.

[17] "REDT Wins £3.6m DECC Award for Energy Storage." *REDT Renewable Energy Storage*. Web. 10 Mar. 2015. <http://www.redtenergy.com/news/redt-wins-£36m-decc-award-energy-storage>.

[18] "REDT Energy Storage Applications." *REDT Renewable Energy Storage*. Web. 10 Mar. 2015. <http://www.redtenergy.com/applications>.

[19] "Redox Flow Batteries to Create $190 Million Market in 2020 - Energy Manager Today." *Energy Manager Today*. 9 Dec. 2014. Web. 10 Mar. 2015. <http://www.energymanagertoday.com/redox-flow-batteries-create-190-million-market-2020-0107339/>.

[20] Babita, B. "Vanadium Redox Batteries: Power Storage Systems for Tomorrow." Print.

[21] "60MWh Redox Flow Battery Order." *Energy Storage Report*. 9 July 2013. Web. 10 Mar. 2015.

[22] "Use REDT Energy Storage Systems to Make Renewables More Reliable." *REDT Renewable Energy Storage*. Web. 10 Mar. 2015. <http://www.redtenergy.com/applications/renewable-energy>.

[23] "History of the Redox Flow Battery." *REDT Renewable Energy Storage*. Web. 10 Mar. 2015. <http://www.redtenergy.com/technology/history>.

[24] "REDT - Energy Efficient Vanadium Redox Batteries." *REDT Renewable Energy Storage*. Web. 10 Mar. 2015. <http://www.redtenergy.com/energystorageproducts>.

[25] Laslau, Cosmin. "Quinone Looks to Challenge Flow Battery Incumbents but Project Cost Remains an Issue." *PV-Tech Storage*. 31 July 2014. Web. 10 Mar. 2015. <http://storage.pv-tech.org/guest-blog/quinone-looks-to-challenge-flow-battery-incumbents-but-project-cost-remains>.

[26] Leung, Puiki, Xiaohong Li, Carlos Ponce De León, Leonard Berlouis, C. T. John Low, and Frank C. Walsh. "Progress in Redox Flow Batteries, Remaining Challenges and Their Applications in Energy Storage." *RSC Advances* (2012). Print.

[27] Spiegel, Colleen. *Designing & Building Fuel Cells*. 1st ed. McGraw-Hill Professional, 2007. 227. Print.

[28] Spiegel, Colleen. *Designing & Building Fuel Cells*. 1st ed. McGraw-Hill Professional, 2007. 230. Print.

[29] Web. 10 Mar. 2015. <http://ocw.mit.edu/courses/chemical-engineering/10-626-electrochemical-energy-systems-spring-2011/lecture-notes/MIT10_626S11_lec03.pdf>.

[30] "Redox Reactions." *Redox Reactions*. Web. 10 Mar. 2015.

<http://www.chemistry.wustl.edu/~coursedev/Online tutorials/Redox.htm>.

[31] Web. 10 Mar. 2015. <http://ocw.mit.edu/courses/chemical-engineering/10-626-electrochemical-energy-systems-spring-2011/lecture-notes/MIT10_626S11_lec01.pdf>.

[32] "Redox Flow Batteries." *Redox Flow Batteries*. Web. 10 Mar. 2015. <http://energystorage.org/energy-storage/technologies/redox-flow-batteries>.

[33] Kumar, R. Vasant, and Thapanee Sarakonsri. "Introduction to Electrochemical Cells." Web. <http://www.wiley-vch.de/books/sample/3527324070_c01.pdf>.

[34] "Batteries: Electricity Though Chemical Reactions." - *Chemwiki*. Web. 10 Mar. 2015. <http://chemwiki.ucdavis.edu/Analytical_Chemistry/Electrochemistry/Voltaic_Cells/Case_Study:_Battery_Types/Batteries:_Electricity_though_chemical_reactions>.

[35] "A Guide to Understanding Battery Specifications." (2008). MIT Electric Vehicle Team. Web. <http://web.mit.edu/evt/summary_battery_specifications.pdf>.

[36] Krebs, Robert E. *The History and Use of Our Earth's Chemical Elements a Reference Guide*. Westport, Conn.: Greenwood, 1998. Print.

[37] Kołodziejczak-Radzimska, Agnieszka. "Zinc Oxide—From Synthesis to Application: A Review." (2014). Web.

[38] "Sodium Dodecyl Benzene Sulphonate (SDBS, LAS)." *Sodium Dodecyl Benzene Sulphonate; LAS; SDBS; Alkylaryl Sulfonate; Alkyl Benzenesulfonic Acid Sodium Salt*. Web. 10 Mar. 2015. <http://www.irochemical.com/product/Surfactants/LAS.htm>.

[39] Rodriguez, Ferdinand. "Plastic." *Encyclopaedia Britannica*. Web. <http://www.britannica.com/EBchecked/topic/463684/plastic>.

[40] Larsson, Annika. "Evaluation of Flow Battery Technology: An Assestment of Technical and Economic Feasibility." (2009). Annika Larsson. Web. <http://dspace.mit.edu/bitstream/handle/1721.1/54555/567548912.pdf?...1>.

Appendices

Appendix A: Plate Dimension

The following diagram shows a two-dimension detailed drawing of the cross sectional dimension of the plate.

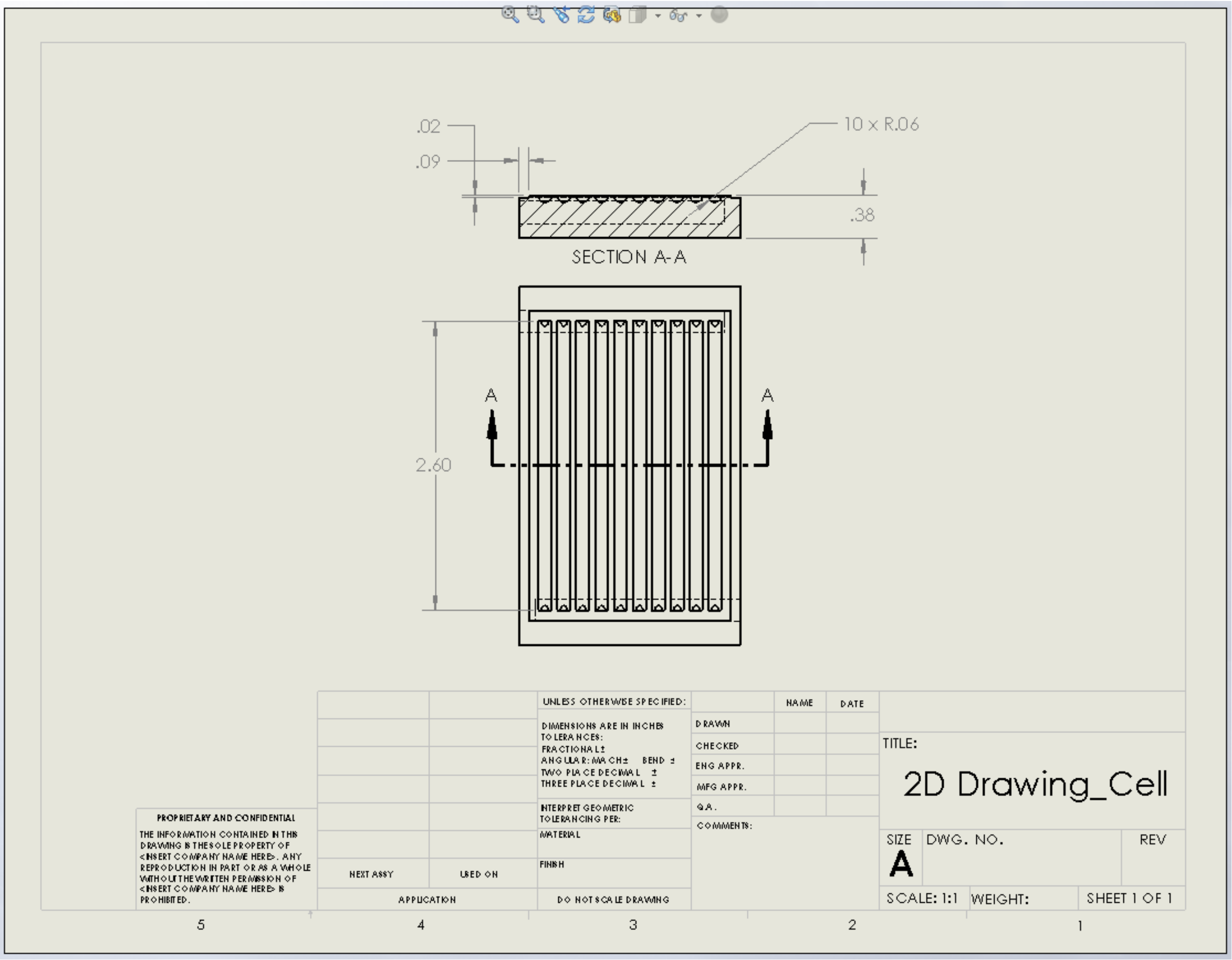

Appendix B: Assembling the Battery

The first picture shows the Copper Charge Plate and the second picture shows the Nickel Charge Plate.

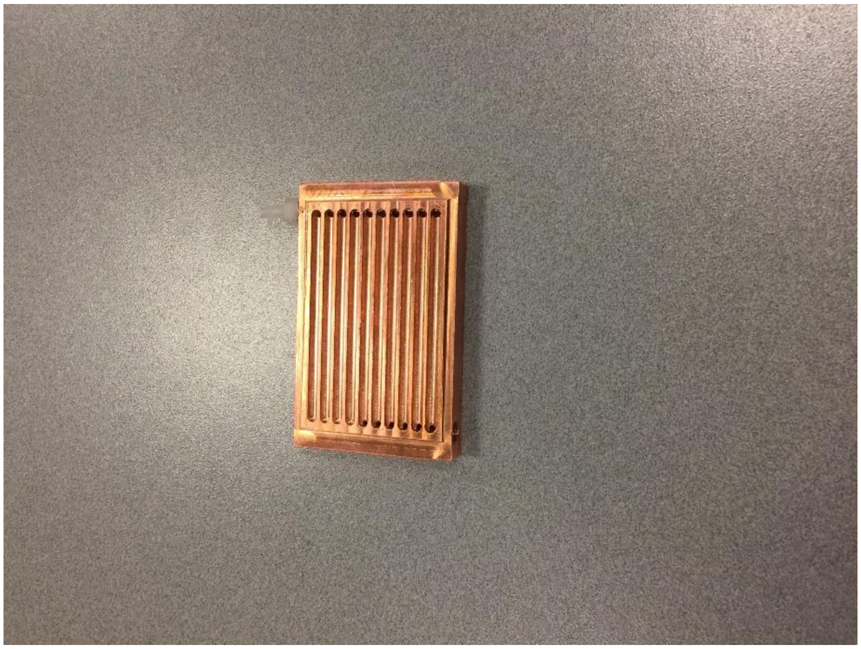

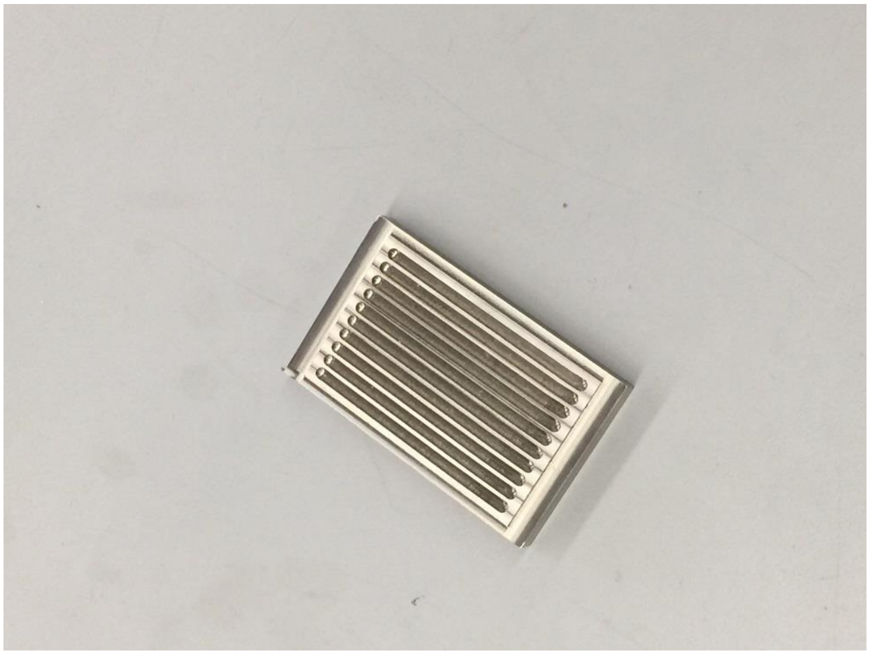

The following figure shows the separator between the electrodes and the flow direction of the cathode and anode slurry.

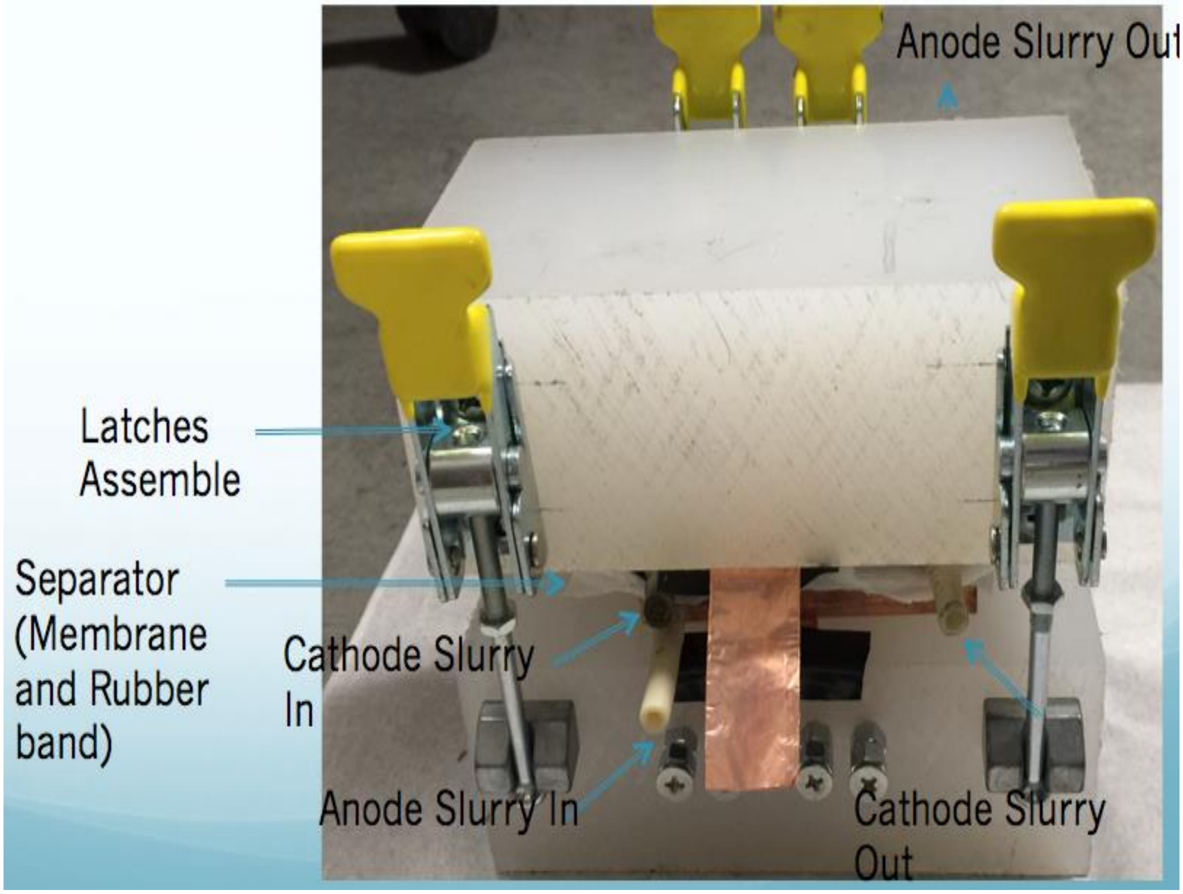

The following figure shows a side view of our prototype.

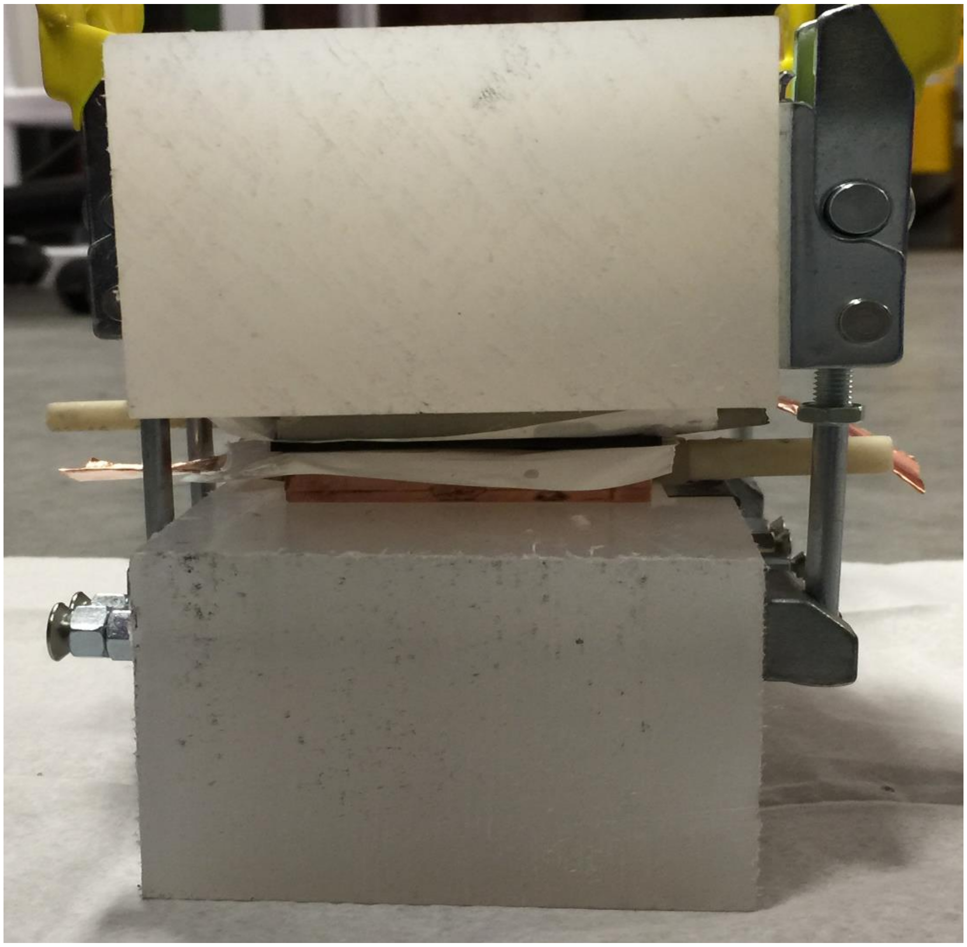

The following figure shows how the holes were sealed using extra tubing material and connectors.

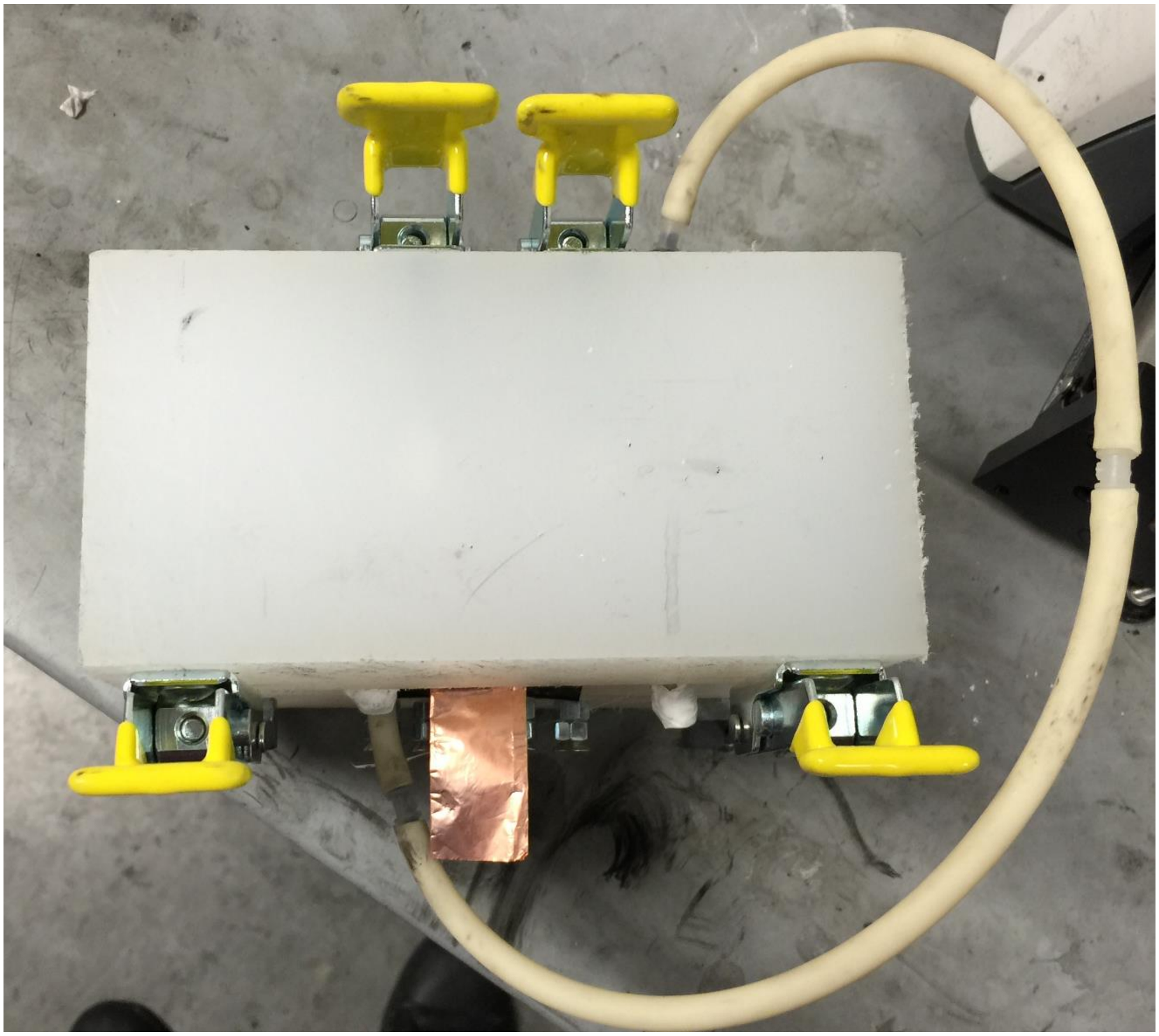

Appendix C: Charge and Discharge Characteristic of the Battery

The following three diagrams show voltage and current relationship against time during the charging and discharging processes.

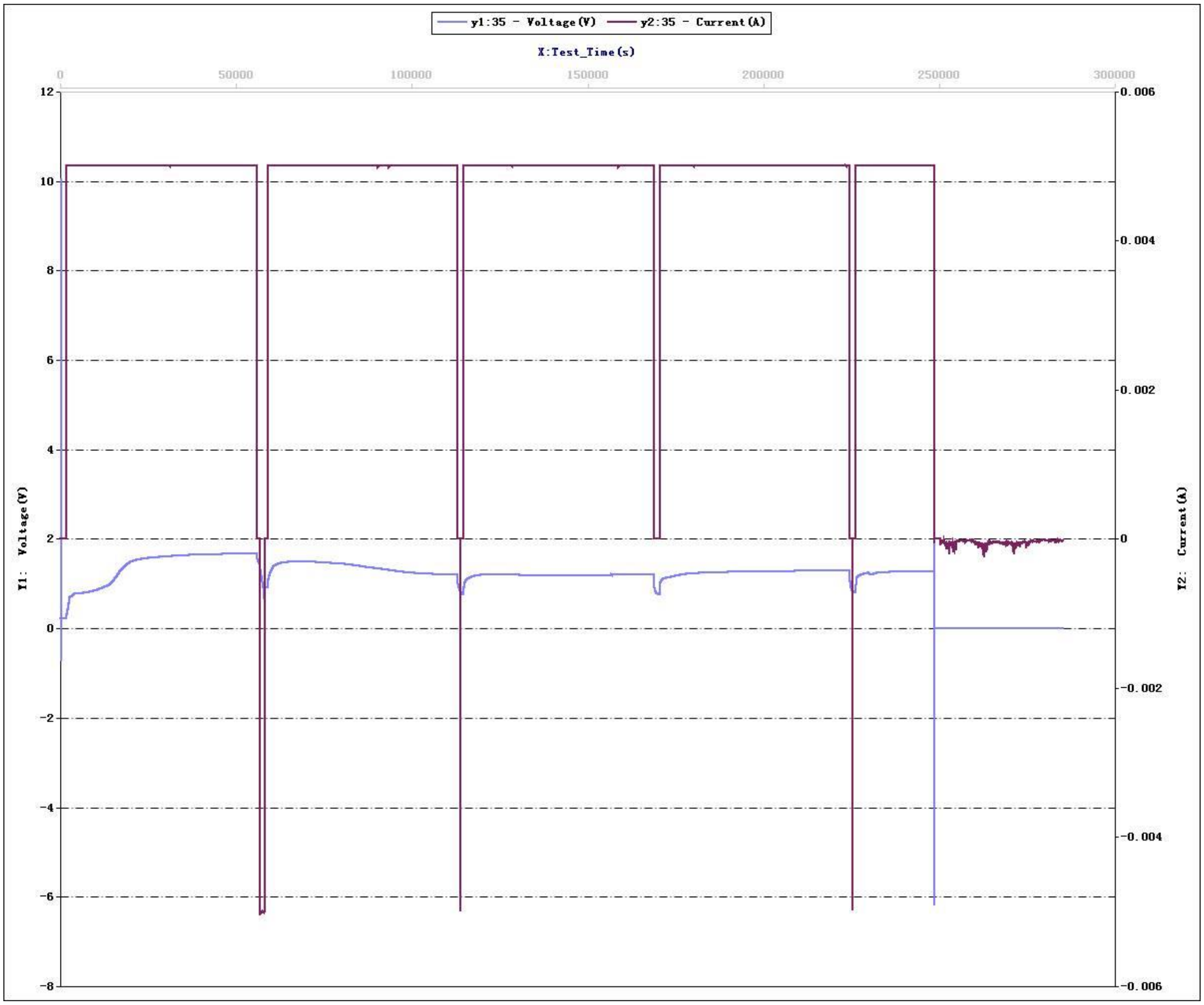

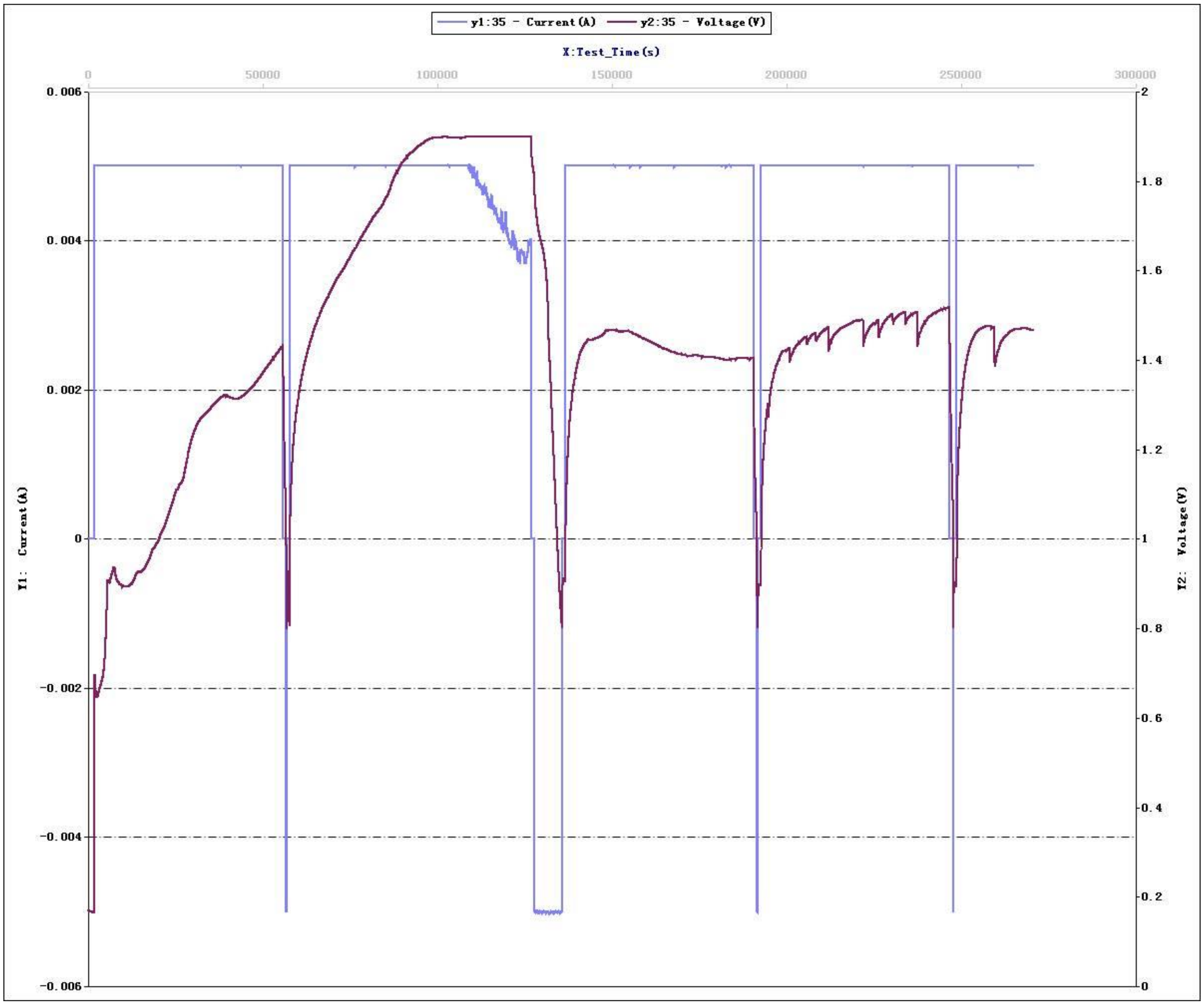
y1:35 - Current(A)
y2:35 - Voltage(V)
X:Test_Time(s)
0
50000
100000
150000
200000
250000
300000
0.006
0.004
0.002
0
-0.002
-0.004
-0.006
Y1: Current(A)
2
1.8
1.6
1.4
1.2
1
0.8
0.6
0.4
0.2
0
Y2: Voltage(V)

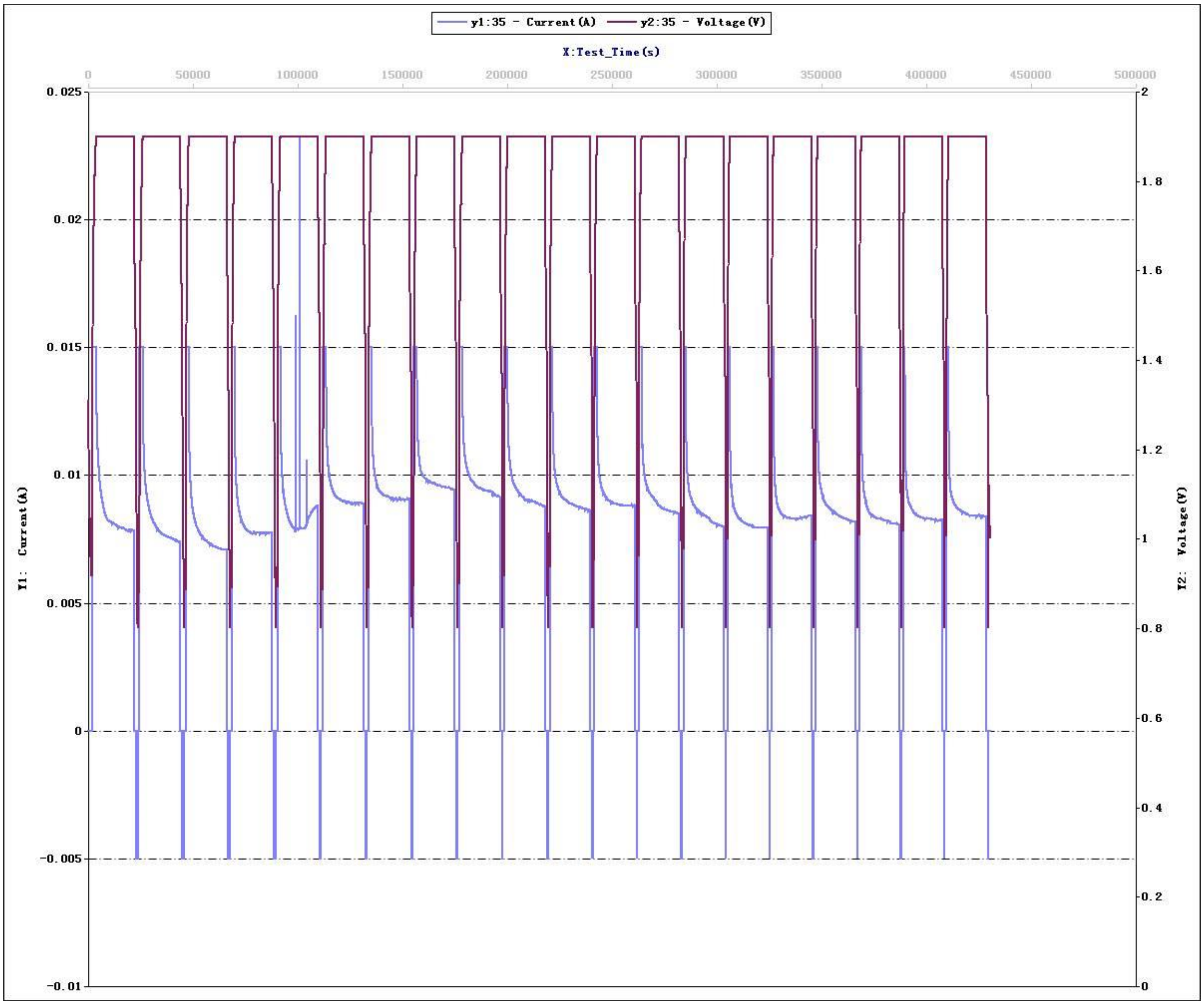
y1:35 - Current(A)
y2:35 - Voltage(V)
X:Test_Time(s)
0
50000
100000
150000
200000
250000
300000
350000
400000
450000
500000
Y1: Current(A)
0.025
0.02
0.015
0.01
0.005
0
-0.005
-0.01
Y2: Voltage(V)
2
1.8
1.6
1.4
1.2
1
0.8
0.6
0.4
0.2
0